We are IntechOpen, the world's leading publisher of Open Access books Built by scientists, for scientists

6,900
Open access books available

186,000
International authors and editors

200M
Downloads

Our authors are among the

154
Countries delivered to

TOP 1%
most cited scientists

12.2%
Contributors from top 500 universities

WEB OF SCIENCE™

Selection of our books indexed in the Book Citation Index in Web of Science™ Core Collection (BKCI)

Interested in publishing with us?
Contact book.department@intechopen.com

Numbers displayed above are based on latest data collected.
For more information visit www.intechopen.com

Chapter 5

Heterostructures Based on Porphyrin/Phthalocyanine Thin Films for Organic Device Applications

Marcela Socol, Nicoleta Preda, Anca Stanculescu, Florin Stanculescu and Gabriel Socol

Additional information is available at the end of the chapter

http://dx.doi.org/10.5772/67702

Abstract

Multilayer or blend heterostructures based on porphyrins and phthalocyanines were obtained on different substrates using VTE and MAPLE methods. Stacked structures based on ZnPc and C60 with NTCDA were prepared by VTE on ITO/glass, their current value being increased by the deposition of the materials in an inverted configuration or by using ITO/PEDOT:PSS as a substrate. Multilayer structures comprising ZnPc and NTCDA were fabricated by MAPLE on an AZO/glass. Treating the AZO in oxygen plasma, a higher current value was obtained for the deposited heterostructures. The oxygen plasma treatment can increase the work function of the AZO resulting in a decrease of the energetic barrier from AZO/organic interface and finally improving the charge transport. Stacked layers or blend heterostructures having ZnPc, MgPc and TPyP were deposited by MAPLE on ITO/PET. In the case of those containing MgPc and TPyP, an increase in the current value (in dark) was obtained for the blend compared to the stacked layer configuration. For those with ZnPc and TPyP, under illumination, a photovoltaic effect was observed for the blend structure. All heterostructures are featured by a large absorption in the visible domain of the solar spectrum and suitable electrical properties for their use in OPV applications.

Keywords: ZnPc, TPyP, MgPc, VTE, MAPLE

1. Introduction

During the last years, the organic materials have attracted the attention of researchers because they can be used in different types of applications: organic photovoltaic (OPV) cells, organic-based light-emitting devices (OLEDs) and organic field effect transistors (OFETs) [1–6]. Heliatek reports a conversion efficiency of about 13.2% for an OPV fabricated by vacuum

INTECH
open science | open minds

© 2017 The Author(s). Licensee InTech. This chapter is distributed under the terms of the Creative Commons Attribution License (http://creativecommons.org/licenses/by/3.0), which permits unrestricted use, distribution, and reproduction in any medium, provided the original work is properly cited. CC BY

evaporation and having three absorbers [7]. OLEDs are already integrated in commercially available devices such as mobile phone displays, TV sets, etc.

The field of organic materials for applications in photovoltaic cells has begun in 1906 and 1913 with the observation of the anthracene photoconductivity [8, 9]. Kearns introduced, in 1958, the first organic photovoltaic cell with a film based on magnesium phthalocyanine (MgPc) [10]. In 1986, Tang makes a step forward for the OPV, fabricating a photovoltaic cell with two organic layers in configuration donor/acceptor (D/A) using copper phthalocyanine (CuPc) as a donor and perylenediimide (PDI) as an acceptor [11]. Since then the photovoltaic effect (PV) was reported in different organic compounds such as porphyrins, phthalocyanines or their derivatives [12]. The organic materials are part from the third generation of photovoltaic, after those based on inorganic materials (the first and second generation).

Comparatively with the inorganic compounds, the organic materials present the following advantages: they can be deposited at low temperature (decreasing in this way the processions costs), are compatible with plastic substrates (a good premise for the flexible electronics) and their properties can be tuned by various processing techniques which allow their deposition even on a large area. In photovoltaic cells, organic compounds present absorption coefficients greater than 10^5 cm^{-1} allowing an increased absorption of the incident light even under 100 nm [13]. The light collection efficiency is dependent on the organic active layer thickness and the absorption properties of the used materials [14].

Porphyrins and phthalocyanines are the most used organic compounds as active layers in photovoltaic cells due to their several absorption maxima in the visible part of the solar spectrum (less than 700 nm [14, 15]). Furthermore, in the porphyrins and derivatives, the range of absorption spectrum in the near infrared part can be increased due to the extended conjugation [14].

The impact of the porphyrins and phthalocyanines on the OPV domain can be evaluated, as shown in **Figure 1**, which contains the histograms with the publications number (from ISI web of science) from the last 5 years (2012 to 2016) having as subject porphyrins or phthalocyanines

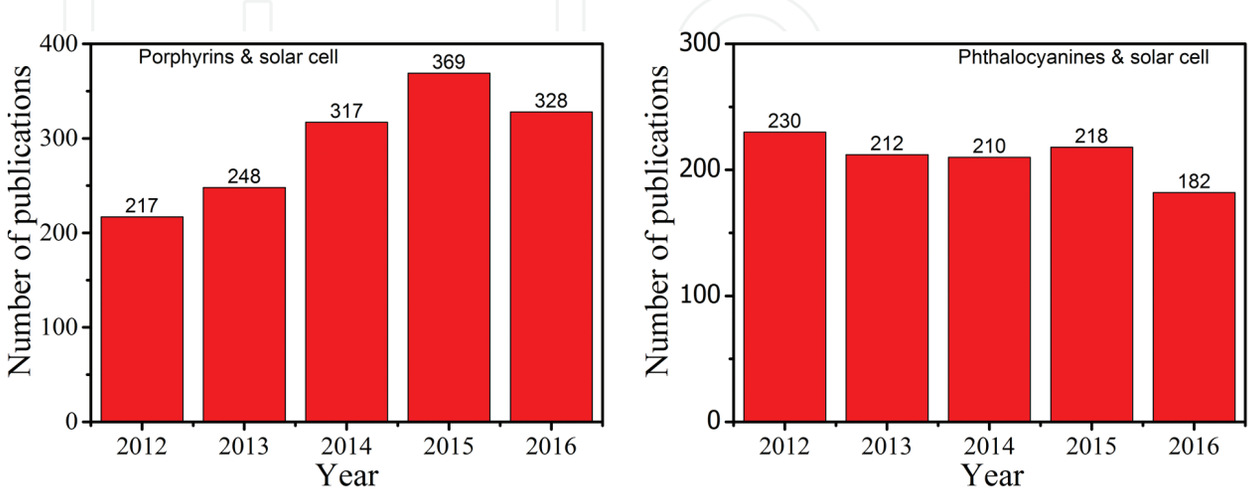

Figure 1. Number of publications per year in the last five years having as topic porphyrins or phthalocyanines and solar cell.

http://dx.doi.org/10.5772/67702

and solar cells. Moreover, it has to be mentioned that there is a journal entirely dedicated to these organic compounds.

Photovoltaic cells based on porphyrins with high performances were achieved. Thus, in 2011 Yella et al. reported 12.3% efficiency for a structure with a zinc porphyrin (YD2-oC8) co-sensitised with Y123 deposited on a TiO_2 [16]. Also, in 2014, a conversion efficiency of about 13% was obtained for a porphyrin dye, coded SM315 [17]. In 2015, a teoretical study made for a new porphyrin-based molecular complex shows that an open circuit voltage of about ~1.8 V can be obtained using this kind of materials [18].

Additionally, the bioinspired structures of porphyrins can be attractive in different forms (nanoparticles, nanosheets, nanorods and nanorings, nanowires, nanotubes, aggregates) as summarised by Monti et al. [19] in applications as catalysts (for O_2 reduction or H_2O oxidation [20]), sensors [21], in photodynamic therapy as photosensitizers [22], for drug delivery [23] and for the treatment of tumours [24].

One of the most important advantages of the phthalocyanines over other organic materials is their increased value of the exciton diffusion length, which is usually in the range of 10 nm [25]. Thus, for CuPc a diffusion length of about ~68 nm was reported [26]. Increased cell performances (efficiency) were also recorded for the OPV based on phthalocyanines: 3.6% for a double layer cell with CuPc and C60 [27], 4.2% for a structure with 1,4,8,11,15,18,22,25-octahexylphthalocyanine ($C6PcH_2$) and [6,6]-phenyl-C61 butyric acid methyl ester (PCBM) prepared by spin-coating [28], 5% for a cell also with CuPc:C60 [29] and the highest reported efficiency of about 5.7 % was achieved also for a structure based on CuPc and C60 [30]. And in the field of the perovskite cells was reported an increased efficiency (11.75%) for a structure containing a ZnPc thin film as a donor material [31].

Complementary, the phthalocyanines and their derivatives have wide range of applications such as OLEDs, gas sensors and optical communications [32]. These compounds are promising candidates in the non-linear optical devices due to their large third-order non-linearity [32, 33]. They are also used in therapy of cancer, infectious or neurodegenerative diseases [34] and in the xerographic photoreceptors of laser printers due to the strong Q-band absorption [35].

In this chapter, we summarised some of our results regarding the preparation and characterisation of porphyrins and metallic phthalocyanine layers for applications in OPV. These materials were obtained as thin films (in multilayer structures or blends) on solid (glass coated with indium tin oxide-ITO or aluminium-doped zinc oxide-AZO) or on a flexible substrate (polyethylene terephthalate-PET coated with ITO).

2. Deposition techniques for single and multilayer thin films: description and advantages

In the applications such as OPV or OLED, the heterostructures consist in one or more organic thin films (active material) sandwiched between two electrodes, an anode that must be transparent (in order to pass the light) and the metallic cathode [13].

The transparent electrode can be prepared by several techniques: sol-gel, magnetron sputtering, oxygen ion beam assisted deposition, pulsed laser deposition (PLD), spray pyrolysis. The widely used methods are RF magnetron sputtering and PLD because films obtained by using these methods are characterised with adequate properties [36, 37].

In the case of the organic compounds, vacuum thermal evaporation (VTE) was one of the most used deposition techniques. Other methods such as spin-coating, doctor blading or inkjet printing were also involved in the preparation of the organic layers [38–40].

The techniques used to prepare our organic heterostructures based on porphyrins and phthalocyanines are briefly described in the following section.

2.1. Transparent conductive oxide (TCO) thin films obtained by pulsed laser deposition (PLD)

PLD is a versatile deposition method frequently used for the preparation of the thin films based on TCO materials [41]. The depositions are made inside a vacuum chamber. A solid target comprising the raw materials is ablated under a pulsed laser beam. When the elements from the target reach their evaporation temperature (above a certain value of the laser intensity), they are ejected from the target and form the plasma plume and pass to the deposition support starting the nucleation process which leads to the formation of the thin layer [42]. In order to improve the properties of the layers, the deposition can be also made in inert gases such as nitrogen (N_2) or in reactive gas such as oxygen (O_2). Also, the deposition target can be rotated during the deposition process to avoid a local deterioration which can affect the uniformity of the obtained film. The deposition parameters that must be controlled are fluence of the laser beam, a number of the laser pulses, target-substrate distance and, sometimes, substrate temperature [41].

High-quality TCO materials with an increased transmittance, low electrical resistivity and a reduced roughness of layer surfaces are obtained by PLD [37, 43].

2.2. Organic thin films prepared by vacuum thermal evaporation (VTE)

VTE is a dry technique, frequently used for the deposition of the metallic layers, inorganic materials but also for the organic compounds. The method is simple and it can be applied for deposition on a large scale being used in the industry. Heliatek fabricated a cell made with three organic layers and high efficiency by VTE [7].

The solubility is another reason for choosing this deposition method which does not imply a solvent, if the organic materials are insoluble or poorly soluble. Thus, can be deposited successive organic layers, the previous deposited layer not being affected by the deposition of the next layer.

Using this method, materials can be evaporated which are vacuum compatible and chemically stable up to their evaporation temperature. In the vacuum evaporation, the material of

http://dx.doi.org/10.5772/67702

interest is heated until its vapour pressure is greater than 10^{-2} Torr [44]. The high vacuum in the deposition chamber ensures a particles flow (atoms, molecules) from the evaporated material. The process is followed by the condensation of the formed vapours on an adequate substrate [45]. As deposition substrates can be used glass, quartz, silicon, ITO or other plate materials.

The evaporation and condensation of the materials are influenced by the following parameters: temperature of the heater (influences the evaporation rate), evaporation rate (depends by the system geometry), substrate temperature (control the surface atom mobility), heater and substrate geometry (related to film uniformity) and substrates (as smooth and clean as possible) [44]. All these parameters are very important because they affect the quality of the obtained thin film. It is known that the thin films have the tendency to copy the form of the substrate used for deposition.

The organic compounds adequate to be deposited by vacuum evaporation are those from the small molecules class, because they do not suffer stoichiometric changes during the transfer, having low melting temperatures (~300°C).

A disadvantage of this method is the time necessary until it is reached the high vacuum in the deposition chamber. But the thin films obtained are uniform, have a good adherence and have the wished geometry (shadow mask being used) [46].

2.3. Organic thin films prepared by matrix-assisted pulsed laser evaporation (MAPLE)

MAPLE is a laser technique that has been developed from the PLD method. It was developed at the end of the 1990s from the necessity to deposit soft organic thin films (unicomponent layers or blends) preserving the properties of the used raw materials. MAPLE is also useful in the deposition of the polymers when the use of VTE results in the broken of the molecular chains [47, 48]. It is also used for the deposition of thin films from small molecule compounds or oligomers [49, 50].

In order to avoid the deterioration of the organic materials during the deposition were used lower laser fluences (<500 mJ/cm^2) compared to those used in the classical PLD [47] and targets (frozen in liquid nitrogen) formed from a mixture between the organic material and an adequate solvent used as a matrix [47, 48]. The solvent is chosen in order to obtain homogeneous mixture with the organic material and to be compatible with the laser wavelength. The solvent evaporation takes place at the absorption of the laser energy that is converted in thermal energy. Further, the solvent is pumped outside from the deposition chamber by the vacuum system [48]. The material of interest reaches the support where the nucleation process starts and the thin layer is formed. The concentration of the target is usually ~3%, depending on the material type.

Multilayer organic heterostructure can be fabricated by MAPLE, because the second deposited layer does not affect the first obtained layer [51].

3. Organic heterostructures with single and multilayer thin films: influence of the deposition technique type on their structural, morphological and optical properties

Different organic heterostructures were obtained either by VTE or MAPLE on a solid glass substrate (covered with ITO or AZO) and on a flexible substrate (covered with ITO). The prepared layers and heterostructures were investigated by various techniques: X-ray diffraction (XRD), atomic force microscopy (AFM), ultraviolet–visible (UV–VIS) spectroscopy, photoluminescence spectroscopy (PL) and infrared Fourier transform spectroscopy (FTIR). The used organic materials were metal phthalocyanines (ZnPc or MgPc), porphyrins (15,10,15,20-tetra(4-pyridyl)-21H,23H-porphine -TPyP) or other small molecule compounds (1,4,5,8-naphthalenetetracarboxylic dianhydride—NTCDA, fullerene-C60), and their chemical structure is presented in **Figure 2**.

3.1. Heterostructures based on ZnPc and NTCDA thin films obtained by VTE and MAPLE

Phthalocyanines are materials that are often used in OPV due to their large absorption domain in the visible part of the spectrum. These compounds are characterised by a high chemical stability having the property to form uniform layer on different solid substrates [52]. Thus, they can be easily deposited by the VTE method.

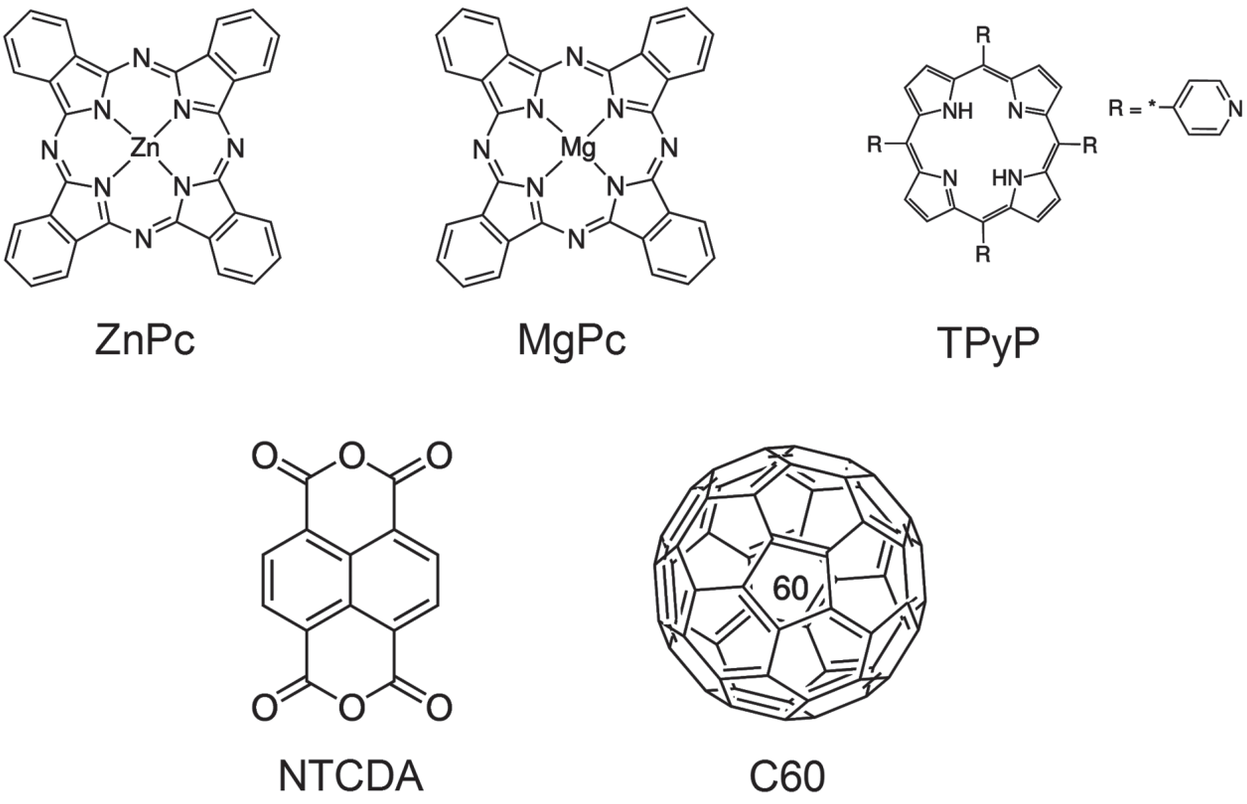

Figure 2. Chemical structure of the ZnPc, MgPc, TPyP, NTCDA and C60.

http://dx.doi.org/10.5772/67702

ZnPc, C60 and NTCDA layers were deposited by the VTE technique [53] on a ITO/glass, poly(3,4-ethylenedioxythiophene)-poly(styrenesulfonate)-PEDOT:PSS/ITO/glass, silicon and glass using the following experimental conditions: 8×10^{-6} mbar pressure in the chamber, at ~218°C for ZnPc, ~255°C for C60 and ~166°C for NTCDA. A PEDOT:PSS layer (20 nm) was prepared by spin-coating on ITO (15 Ω/sq) at a rotation speed of 3000 rot/min for 30 s. After that the obtained layers were supposed to a thermal treatment at 120°C for 5 min [53].

The following heterostructures were fabricated: 1-[(ITO/ZnPc(50 nm)/C60(30 nm)/NTCDA(110 nm)/Al)], 2-[(ITO/PEDOT:PSS(20 nm)/ZnPc(50 nm)/C60(20 nm)/NTCDA(120 nm)/Al)] and 3-[glass/Al/NTCDA(90)/C60(20)/ZnPc(50)/ITO]. For the second type of heterostructure (starting from glass/Al), the ITO electrode (the last material deposited) was prepared by PLD with an excimer laser source (λ = 248 nm and τ_{FWHM} ~25 ns) using the following experimental conditions: room temperature, 5 Hz repetition rate, 30,000 number of laser pulses, in oxygen atmosphere at 1.5 Pa pressure [53]. The resistivity of ITO was 3.9×10^{-4} Ωcm. Aluminium was used as a top metallic electrode (80 nm) being also obtained by VTE at 10^{-4} Pa pressure in the deposition chamber. The schematic representations of the prepared organic heterostructures are given in **Figure 3**.

The XRD diffractograms (**Figure 4**) indicated that the organic films obtained by VTE are not completely amorphous. The ZnPc layer presents lower diffraction peaks at 6.9, 9.6 and

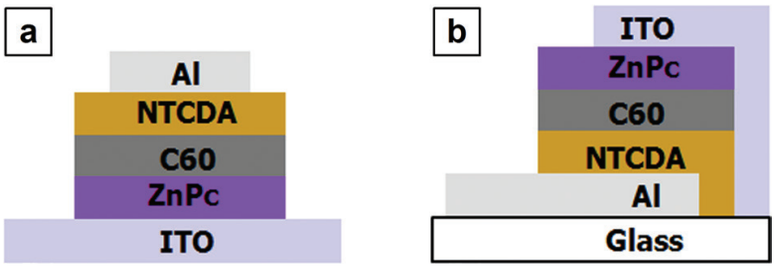

Figure 3. Schematic representation of the organic heterostructures deposited by VTE: standard structure (a) and inverted structure (b).

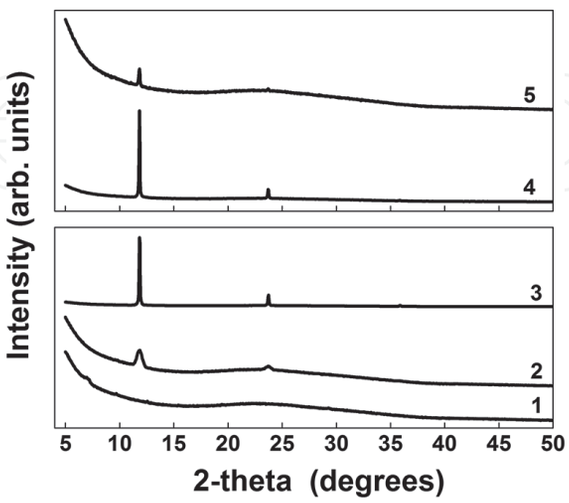

Figure 4. XRD patterns of the ZnPc film (curve 1), C60 film (curve 2), NTCDA film (curve 3), standard structure (curve 4) and inverted structure (curve 5) deposited by VTE.

29.3° [29], attributed to the powder raw material [54]. For the C60 layer, remarked lines were obtained at 11.8 and 23.7° specific to the (111) and (311) diffraction plane of this material [55]. The XRD diagram of the NTCDA film presents three peaks, including an intense one at 11.9° obtained also in the diffractogram of the powder [53]. Depending on the method used for deposition of the organic layers, in the multilayer structures are remarked only the diffractions lines originating from NTCDA, which are more intense when NTCDA is deposited on top (**Figure 4**, curve 4).

For the ZnPc and C60 films, the AFM images (**Figure 5**) show topography characteristic to these materials deposited by thermal evaporation [56, 57]. Thus, it can be observed a low roughness for the ZnPc film (root mean square, RMS = 5.1 nm) in comparison with C60 (RMS = 14.7 nm) and NTCDA (RMS = 20.9 nm). The RMS higher value of the NTCDA can be attributed to the layer thickness, this layer being thicker than ZnPc and C60 films.

For the heterostructures containing three organic layers, a reduced roughness was obtained in the inverted structure (RMS = 6.8 nm) compared to the normal structure (RMS = 8.3 nm) as it is expected, taking into account that in standard structure the top organic layer is NTCDA which is characterised by the highest roughness.

The vibrational properties of the raw materials were identified in the FTIR spectra (**Figure 6**) of ZnPc and NTCDA layers deposited by VTE, indicating that no chemical decomposition took place during the VTE transfer. The C60 film was too thin to remark some FTIR peaks on it. In the ZnPc layer, the peak from 727 cm^{-1} is specific to C-H out of plane deformation, the peaks situated at 748, 1095, 1118 and 1288 cm^{-1} appear due to the in-plane C-H bending, the peak at 1333 cm^{-1} evidenced the C-C stretching in isoindole and the peaks from 1481 to 1608 cm^{-1} are attributed to the C-C stretching in benzene [56, 58].

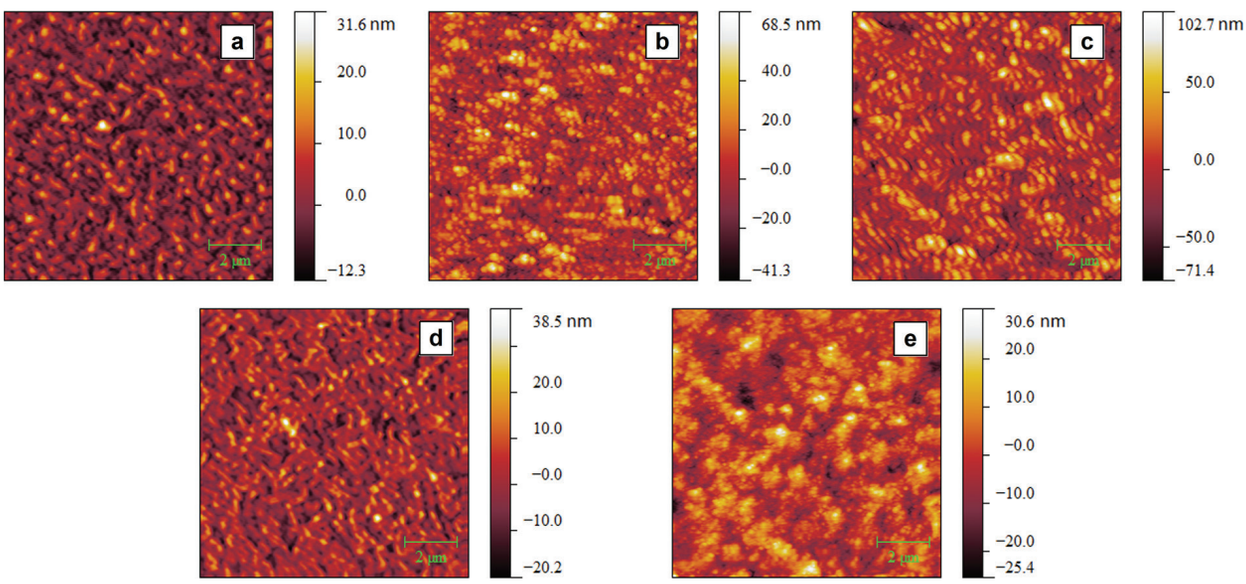

Figure 5. AFM images of the ZnPc film (a), C60 film (b), NTCDA film (b), standard structure (d) and inverted structure (e) deposited by VTE.

http://dx.doi.org/10.5772/67702

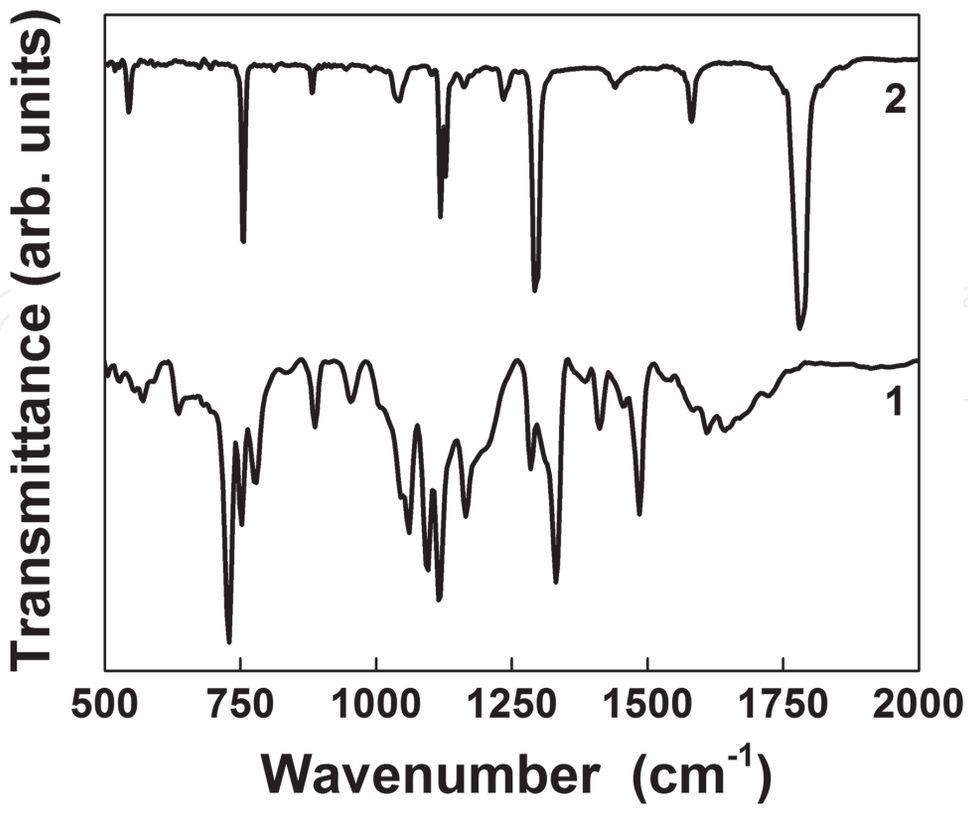

Figure 6. FTIR spectra of the ZnPc (curve 1) and NTCDA (curve 2) single layers deposited by VTE.

For the NTCDA layer, the peaks at 1780 cm^{-1} (characteristic to the dianhidrydecarbonylic group [59]), at 543, 753 and 882 cm^{-1} (specific to the C-H out-of-plane bending vibrations [60, 61]), at 698 and 754cm^{-1} (attributed to C-H bending vibration [36]), at 1044, 1120, 1161, 1234 and 1293 cm^{-1} (characteristic to the stretching vibration of C-O in the anhydride groups and the C-H in-plane bending vibration) and at 1442 and 1582 cm^{-1} due to the C-C bending [61]) were evidenced.

The UV–VIS spectra of the VTE prepared organic thin films are given in **Figure 7**. For the ZnPc layer, a high transparency (~90% at 500 nm) was emphasised, covering a broad part of the VIS region and presenting the band B (so-called Soret band) and band Q [62, 63]. Several absorption maxima are remarked for the C60 layer, at 340, 400 and 440 nm which are characteristic to this material prepared by the VTE technique [64, 65]. The NTCDA layer used as buffer in our structure reveals absorption maxima in UV (at 370 and 390 nm) attributed to the π-π^* transition [66]. The structure comprising all the organic layers (**Figure 7**, curve 4) is characterised by a high transmittance, showing the absorption maxima of all components.

ZnPc, C60 and NTCDA thin films deposited by the VTE method are polycrystalline and have morphologies specific to raw materials (ZnPc, C60 and NTCDA), being characterised by different roughness values (RMS ranged between 5.1 and 20.9 nm). The materials present adequate absorption bands in the visible region. The peaks disclosed by the FTIR spectra are assigned to each organic material, evidencing that no chemical decomposition appears in the thin-film deposition.

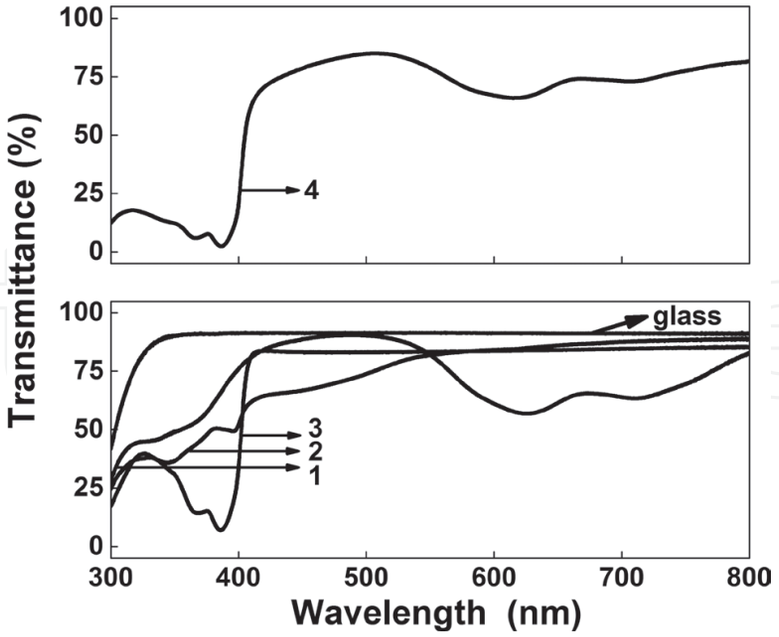

Figure 7. Transmission spectra of the ZnPc film (curve 1), C60 film (curve 2), NTCDA film (curve 3) and standard structure (curve 4) deposited by VTE.

Along the time, ITO was the most used transparent electrode, due to its high optical transmittance and reduced electrical resistivity. Because the required indium is rare and expensive, many attempts were made in order to replace the ITO in various applications, including the OPV field.

As transparent electrode we choose a large band gap semiconductor, ZnO doped with Al (AZO) because it presents adequate electrical resistivity (~10^{-4} Ωcm), a high optical transmission in the visible-NIR domain, and a higher chemical stability in comparison with ITO [67–69].

AZO (ZnO doped with 2% Al) thin films were prepared at room temperature on a glass substrate by PLD using the KrF* excimer laser in the following experimental conditions: 10 Hz repetition rate 5 cm, substrate-target distance, 3 J/cm^2 laser fluence, 32,000 laser pulses, in oxygen atmosphere at 10^{-2} mbar pressure [70]. Subsequently, the obtained AZO layers were treated in oxygen plasma at 0.6 mbar and P_{max} = 130 W (for 5 and 10 min) in order to observe how this treatment affects the properties of the formed layers. The samples were labelled as follows: AZO (untreated film), 5AZO (film treated for 5 min) and 10AZO (film treated for 10 min).

The MAPLE technique was used to process organic films from ZnPc and NTCDA on the AZO substrate. The same laser source was used to prepare thin films from a frozen target containing ZnPc or NTCDA and dimethyl sulphoxide (DMSO) as a solvent compatible with the laser wavelength. Two different laser fluences were used for the deposition of the ZnPc layer: 0.4 J/cm^2 (1ZnPc) and 0.3 J/cm^2 (2ZnPc). Organic heterostructures with two stacked layers were formed by the deposition of the NTCDA layer over ZnPc films. For the NTCDA, the deposition parameters were 0.3 J/cm^2 laser fluence, 90,000 and 100,000 laser pulses [70]. **Table 1** presents the experimental conditions for the deposition of the organic layers.

Sample	ρ of AZO before/after treatment (10^{-4} Ωcm)	Laser fluence (J/cm²)	No. of laser pulses (K)	d/RMS of AZO (nm)	d/RMS of ZnPc (nm)	d/RMS of NTCDA (nm)
AZO/1ZnPc/NTCDA	3.1/3.1	0.4/0.3	65/90	1310/9.3	360/51	120/59
AZO/2ZnPc/NTCDA	2.7/2.7	0.3/0.3	65/90	1300/9.2	380/53	150/73
5AZO/1ZnPc/NTCDA	2.9/2.8	0.4/0.3	65/100	1290/6.4	550/60	140/42
5AZO/2ZnPc/NTCDA	2.9/3.1	03/0.3	65/100	1290/6.1	390/61	90/50
10AZO/1ZnPc/NTCDA	3.1/3.1	0.4/0.3	65/100	960/4.4	490/61	120/53
10AZO/2ZnPc/NTCDA	3.2/2.5	0.3/0.3	65/100	940/3.3	440/60	100/56

Table 1. Resistivity of the AZO layers before and after treatment, used laser fluences in the MAPLE deposition, the thickness (d) of the layers and the roughness value obtained from AFM.

http://dx.doi.org/10.5772/67702

The heterostructures (**Figure 8**) were carried out by the gold (Au) electrode of ~100 nm thickness deposited also by VTE.

The morphological investigations of the AZO substrates and of the ZnPc/NTCDA structures are represented in **Figure 9**. Only the AFM images collected for the structures with the ZnPc layer deposited at 0.4 J/cm^2 laser fluence are presented, but the roughness (RMS) values both for structures with ZnPc deposited at 0.4 and 0.3 J/cm^2 laser fluences are presented in **Table 1**.

Oxygen plasma treatment leads to a decrease in the RMS value of the AZO substrate, from 9.3 nm for the untreated film to 3.3 nm for the treated film for 10 min (**Table 1**). A similar behaviour was remarked by others authors [71]. The AFM images exhibit a topography characterised by small grains for the organic layers obtained on treated substrate compared to that formed on the untreated substrate. The RMS value increases from the single to bilayer structures prepared on the untreated AZO substrate. The RMS recorded for the ZnPc layer shows an increase when the AZO substrate is treated (**Table 1**). Probably, the ZnPc deposition is affected by the surface energy of AZO layer modified during the oxygen plasma treatment. The higher roughness of the ZnPc layer obtained on the AZO-treated substrate leads to a better arrangement of the NTCDA molecules having an effect on lowering the RMS value recorded for the bilayer heterostructures.

From the UV–VIS spectra, a transparency between 75 and 87% in the range 400–800 nm was obtained for the AZO layers (**Figure 10**, curve 1). The thickness of the AZO films was evaluated using the formula from [72] which takes into consideration successive interference maxima and minima. The obtained values (between 940 and 1310 nm) are given in **Table 1**.

The UV–VIS spectra of the AZO layers revealed a slight improvement in the transparency with the increase in duration of the applied plasma treatment (**Figure 10**, curves 1′ and 1′′). This can be attributed either to a reduction of the defects number inside the AZO layer (these can act as scattering centres), due to decrease in the AZO layer thickness (**Table 1**) or to the reduction in scattering at the surface in wavelength domain (>750 nm).

The thickness of the organic films was also estimated from the UV–VIS spectra, using the absorption coefficients at λ = 355 nm reported in the literature, $\alpha_{ZnPc} = 3.5 \times 10^4$ cm^{-1} [73] and $\alpha_{NTCDA} = 2.1 \times 10^5$ cm^{-1} [74]. The thickness varied between 360 and 550 nm for the ZnPc layer and between 90 and 150 nm for NTCDA (**Table 2**).

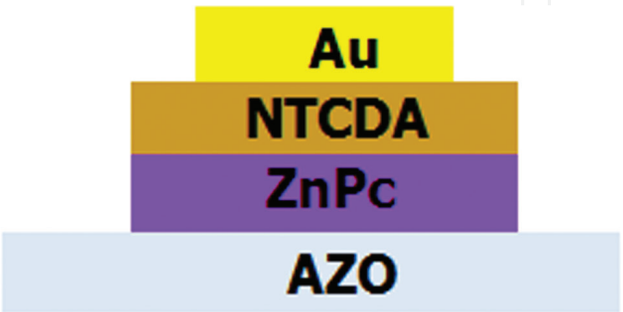

Figure 8. Schematic representation of the organic heterostructure deposited by MAPLE on AZO substrate.

http://dx.doi.org/10.5772/67702

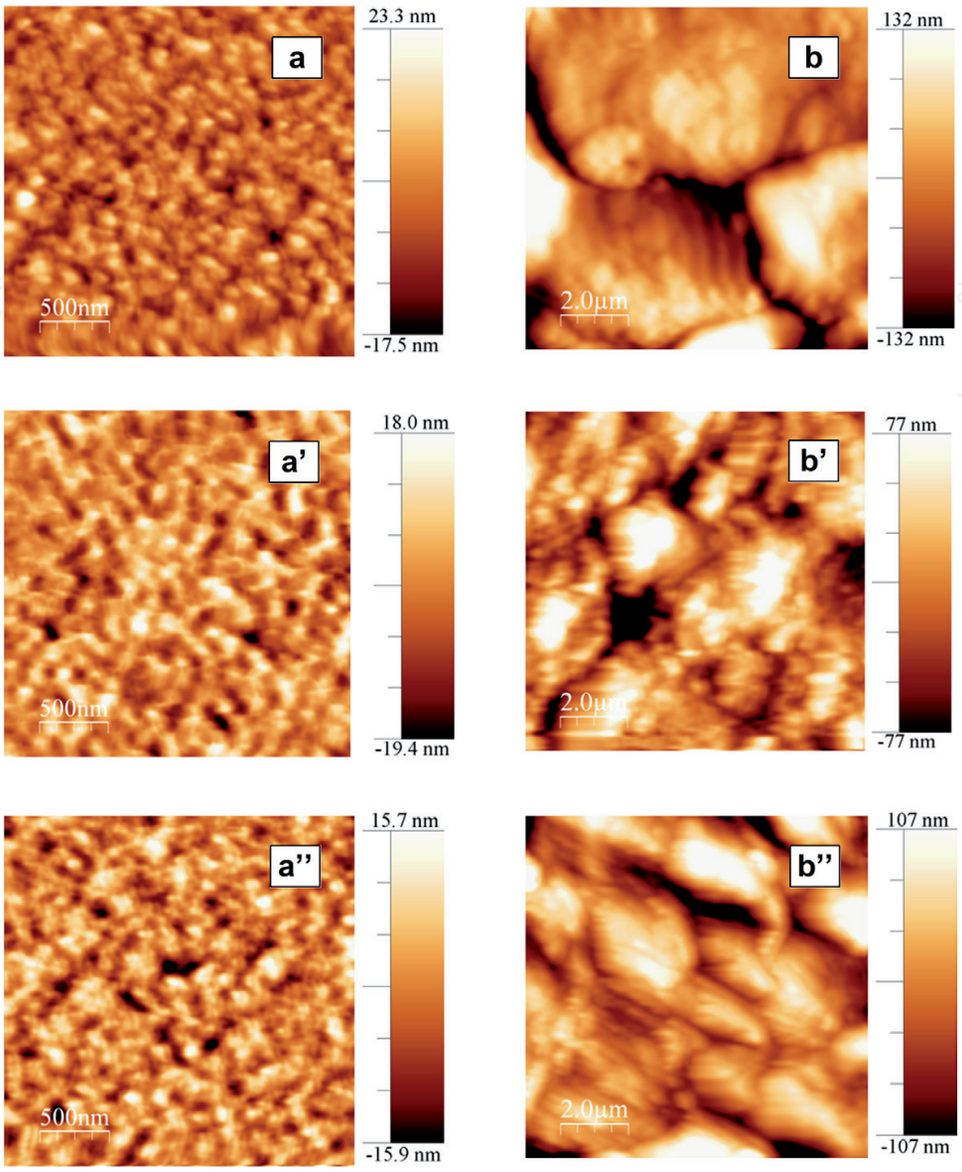

Figure 9. AFM images of the glass/AZO substrates (a, a′ and a′′) and ZnPc/NTCDA layers deposited by MAPLE—0.4 J/cm^2 fluence for ZnPc and 0.3 J/cm^2 fluence for NTCDA (b, b′ and b′′): untreated (a, b), treated in oxygen plasma for 5 minutes (a′, b′) and treated in oxygen plasma for 10 minutes (a′′, b′′).

The ZnPc layers (**Figure 10**, curves 2 and 3) present a structured absorption in the range of 550–750 nm, this large absorption domain being useful in generation of the charge carriers. As mentioned above, the oxygen plasma treatment can modify the surface energy of the AZO layer, can change the way in which the organic molecules are arranged on the substrate and as consequence the optical properties of these organic layers. Comparison of the 1ZnPc and 2ZnPc samples was found that for the second film the absorption is smaller. Additionally, the NTCDA layer does not affect the shape of the transmission spectrum (**Figure 10**, curve 3).

The emission properties of the samples under excitation with λ_{exc} = 335 nm were also investigated (**Figure 11**). The AZO layer is characterised by an intense emission band with maximum at ~430 nm and a shoulder at ~480 nm, linked to point defects as Zn^{2+} interstitial [75, 76].

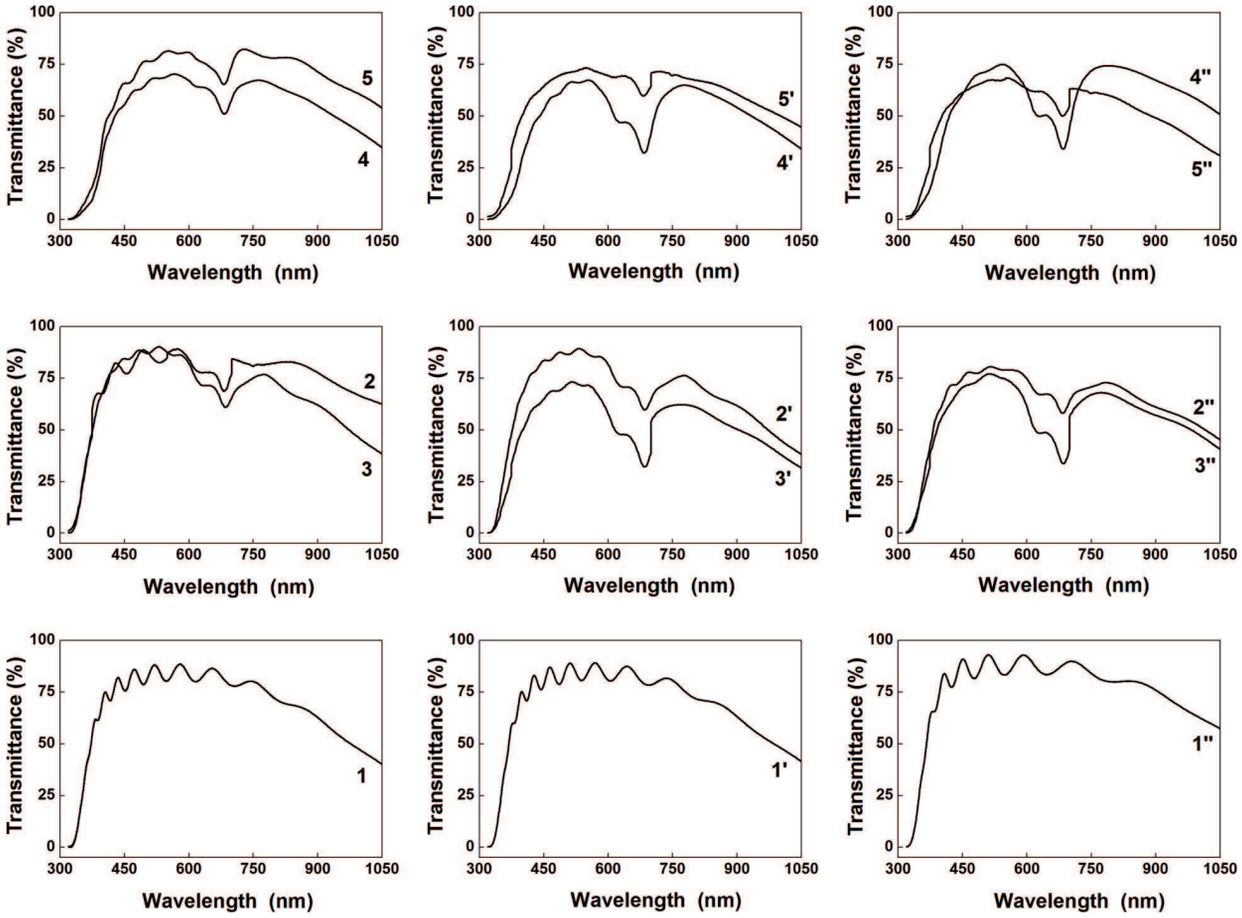

Figure 10. Transmission spectra of the organic films deposited by MAPLE on a glass/AZO substrate untreated (1–5), treated in oxygen plasma for 5 min (1′-5′) and treated in oxygen plasma for 10 min (1″-5″): glass/AZO substrate (curves 1, 1′ and 1″), 1ZnPc film (curve 2, 2′ and 2′′), 2ZnPc film (curve 3, 3′ and 3′′), 1ZnPc/NTCDA layers (curve 4, 4′ and 4′′) and 2ZnPc/NTCDA layers (curve 5, 5′ and 5′′).

Sample	Laser pulses	Thickness (nm)	RMS (nm)
ZnPc/ITO	100k	570	36
MgPc/ITO	85k	470	35
TPyP/ITO	74k	440	34
TPyP/ZnPc/ITO	30k/30k	430	25
TPyP:ZnPc/ITO	60k	380	32
TPyP/MgPc/ITO	30k/30k	530	49
MgPc:TPyP/ITO	60k	440	57

Table 2. MAPLE conditions used for the deposition of organic films and structures on ITO/PET, layer thickness and RMS values interpolated from AFM.

The oxygen radicals from the plasma can lower the number of the Zn^{2+} interstitials due to the reduction of the defects which appear near to the film surface [77]. The thickness of the samples has a decisive role in the intensity of the emission. In the AZO and 5AZO thicker layers, the

http://dx.doi.org/10.5772/67702

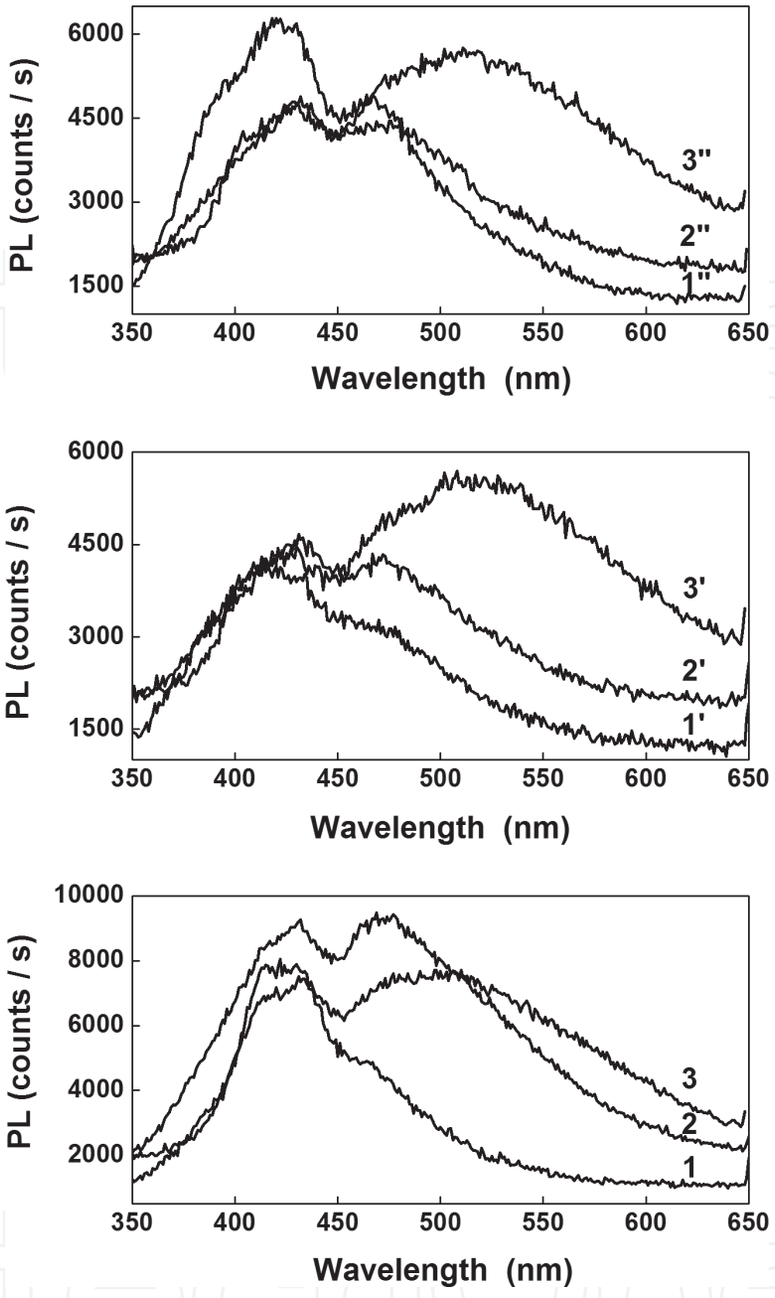

Figure 11. Photoluminescence spectra of the organic films deposited by MAPLE on a glass/AZO substrate untreated (1–3), treated in oxygen plasma for 5 min (1′-3′) and treated in oxygen plasma for 10 min (1″-3″): glass/AZO substrate (curves 1, 1′ and 1″), 1ZnPc film (curve 2, 2′ and 2″) and 1ZnPc/NTCDA layers (curve 3, 3′ and 3″).

emission band attributed to the deep level point defects (2.6 eV) is lower while in the thinner 10AZO layer the emission increases (**Figure 11**, curves 1).

The emission band situated at 430 nm in the AZO spectrum can be remarked also in the structures prepared with ZnPc and ZnPc/NTCDA (**Figure 11**, curves 2 and 3). The ZnPc layer discloses also a peak in the range of 400–450 nm [78]. The shoulder situated at 480 nm from AZO became a well-structured band in the structures containing ZnPc. No supplementary maxima were observed by adding NTCDA, probably because the emission bands specific to this material, one situated at ~430 nm and other situated in 475–575 nm range are masked by

the emission of the AZO and ZnPc layers, respectively [79]. The intensity of the emission band with the maximum at 480 nm from the AZO substrate decreases in the structures prepared with one or two organic layers.

AZO layers were successfully transferred by PLD, in order to be further used to prepare organic heterostructure by MAPLE. The oxygen plasma treatment influences the roughness of the AZO layers. A decrease of the films roughness is obtained with the increase duration of the applied treatment. For this TCO, a high transmittance and emission with maxima at about 430 and 480 nm were evidenced. The organic heterostructures formed on the AZO substrate present also a high transmittance in the visible domain. The surface topography of the organic heterostructures is characterised by grains, smaller grains being remarked for the AZO/1ZnPc/NTCDA structure made on the treated AZO substrate.

3.2. Heterostructures based on metal phthalocyanines (ZnPc or MgPc) and TPyP thin films prepared by MAPLE

Another type of organic heterostructure has bulk active layer. The bulk heterojunction concept [80] was introduced to overpass the mismatch between the energy bands of the constituent organic materials used to form an organic cell with different layers. A bulk heterojunction can be obtained using a wet method for the deposition of the organic materials, these being mixed in a solution with an adequate solvent from which are subsequently deposited films. The organic p-n materials form an interpenetrating network. In this way, the interface between them is enlarged, having effect on the exciton dissociation and the charge transport [81].

The MAPLE method described above was used for obtaining structures with metallic phthalocyanines (ZnPc or Mg Pc) and a non-metallic porphyrin, 5,10,15,20-tetra(4-pyrydil)21H,23H-porphyne (TPyP) as a bulk active layer or as a stacked layer, to investigate the effect of the cell architecture on the properties. In these structures, the phthalocyanines are the p-type material and the TPyP is the n-type material.

A flexible ITO/PET substrate (14 Ω/sq resistivity) was used as a TCO electrode. For the MAPLE deposition, the same above presented laser was involved, keeping the constant experimental conditions: 2.5% concentration of the organic material in DMSO, 300 mJ/cm^2 laser fluence, 5 Hz laser frequency and 5 cm target-substrate distance. In order to obtain layer with appropriate thickness, the number of the laser pulses was varied (**Table 2**). Besides ITO/PET, substrates as a glass and silicon were used. In the structures containing blends, the materials were used in the weight ratio of 1:1 and in those having two stacked layers: the first deposited layer was the metallic phthalocyanine [50]. A schematic representation of the transferred MAPLE layers is presented in **Figure 12**.

The layers prepared were analysed from structural point of view, the diffractograms of ZnPc, MgPc, TPyP and their structures are presented in **Figure 13**. The single layers and the heterostructure based on MgPc are amorphous. In the case of the diffractograms of heterostructures based on ZnPc, some lines characteristic to this material are observed (6.8, 9.1 and 13.8°) [54, 63], meaning that ZnPc presents some degree of crystallinity. The amorphous

http://dx.doi.org/10.5772/67702

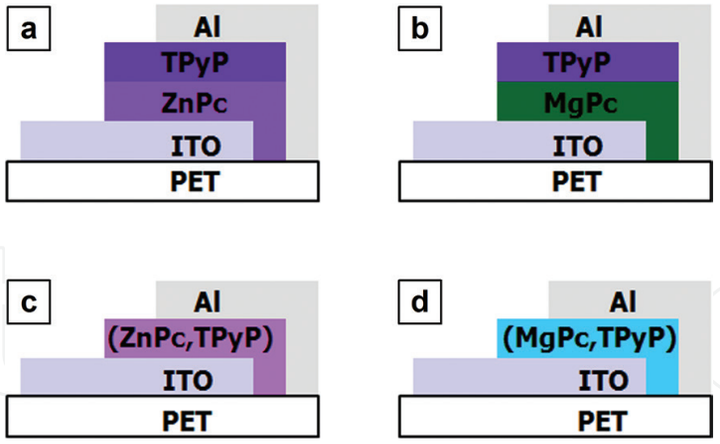

Figure 12. Schematic representation of the organic heterostructures deposited by MAPLE with stacked films (a, b) and mixed layers (c, d).

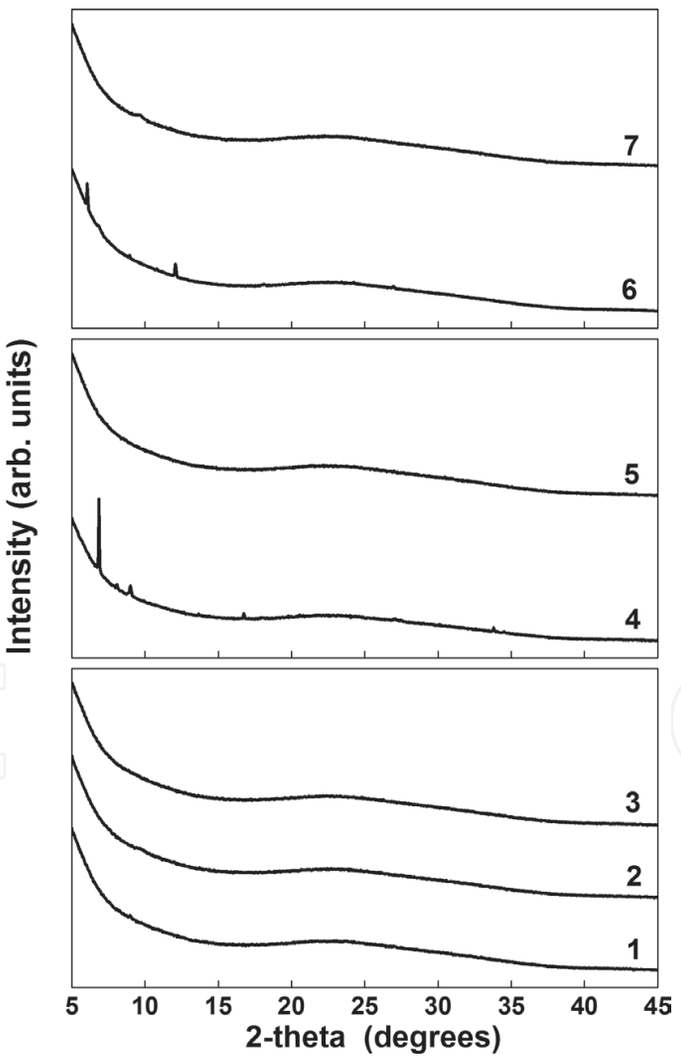

Figure 13. XRD patterns of the organic layers deposited by MAPLE: single layers—ZnPc (curve 1), MgPc (curve 2), TPyP (curve 3), heterostructures containing stacked films—ZnPc/TPyP (curves 4), MgPc/TPyP (curve 5) and heterostructures with mixed layers—ZnPc:TPyP (curves 6), MgPc:TPyP (curve 7).

behaviour of the phthalocyanines was also reported for films prepared by VTE [82]. So, this behaviour is independent of a deposition technique.

The AFM images (**Figure 14**) were recorded on thin films and on the structures. The granular morphology showed by the deposited films was also reported in other papers, this morphology being characteristic to the MAPLE prepared films but also to the phthalocyanines [56, 62, 83]. Small and large grains were disclosed by the AFM images performed on mixed layers (ZnPc:TPyP and MgPc:TPyP). The RMS values extracted from AFM are between 25.0 and 56.8 nm (**Table 2**).

A small RMS value is presented by the TPyP/ZnPc/ITO structure, meaning that in the stacked structure appears a better accommodation of the TPyP molecules on the rough ZnPc film (35.7 nm). The highest RMS value was obtained for the MgPc:TPyP/ITO structure. Probably, the MgPc:TPyP blend is less homogenous in DMSO, the obtained films being characterised by bigger grains comparable with ZnPc:TPyP blend.

The optical properties of the phthalocyanines and porphyrins films were also analysed. The FTIR spectra (**Figure 15**) were recorded in order to observe if some changes appear in the structure of the materials deposited by MAPLE. Thus, the FTIR spectra of the films are shown in comparison with those of the raw powders, the IR bands from the powders appearing also in the thin films, with lower intensity (due to the film thickness). In the phthalocyanines, films

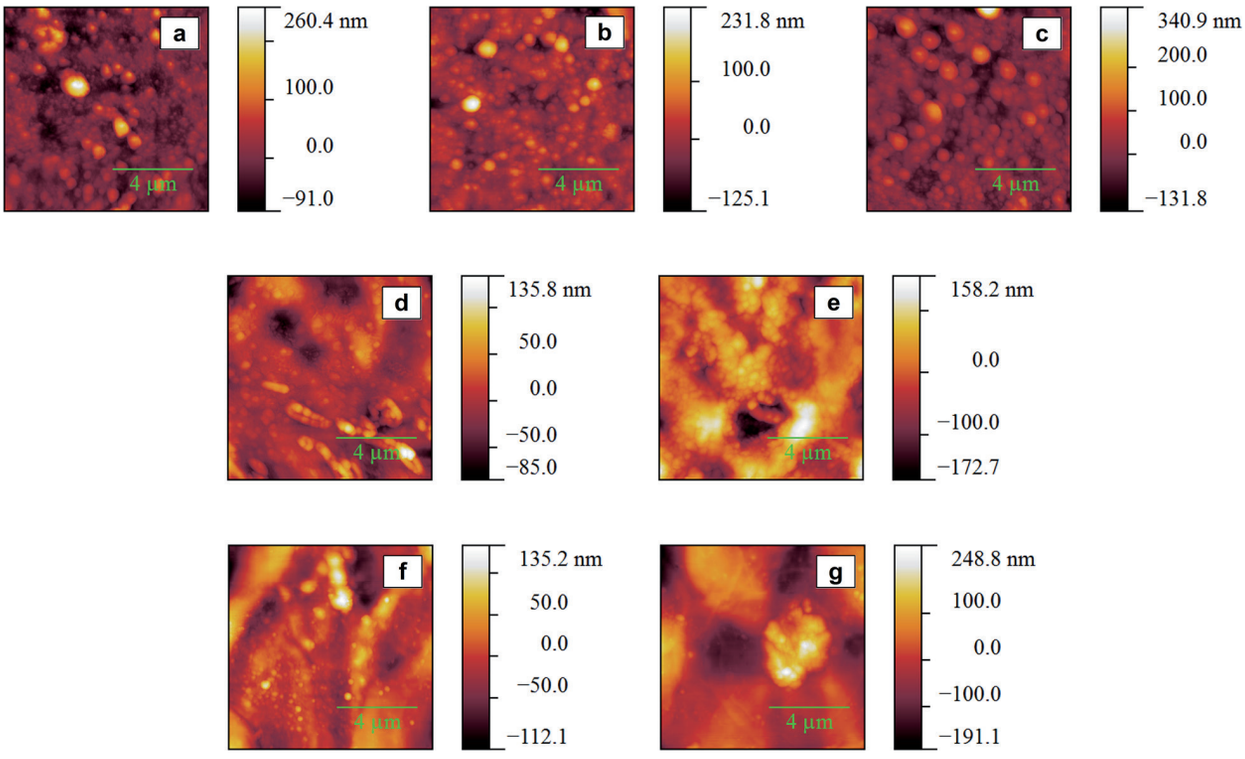

Figure 14. AFM images of the organic layers deposited by MAPLE: single layers—ZnPc (a), MgPc (b), TPyP (c), heterostructures containing stacked films—ZnPc/TPyP (d), MgPc/TPyP (e) and heterostructures with mixed layers—ZnPc:TPyP (f), MgPc:TPyP (g).

http://dx.doi.org/10.5772/67702

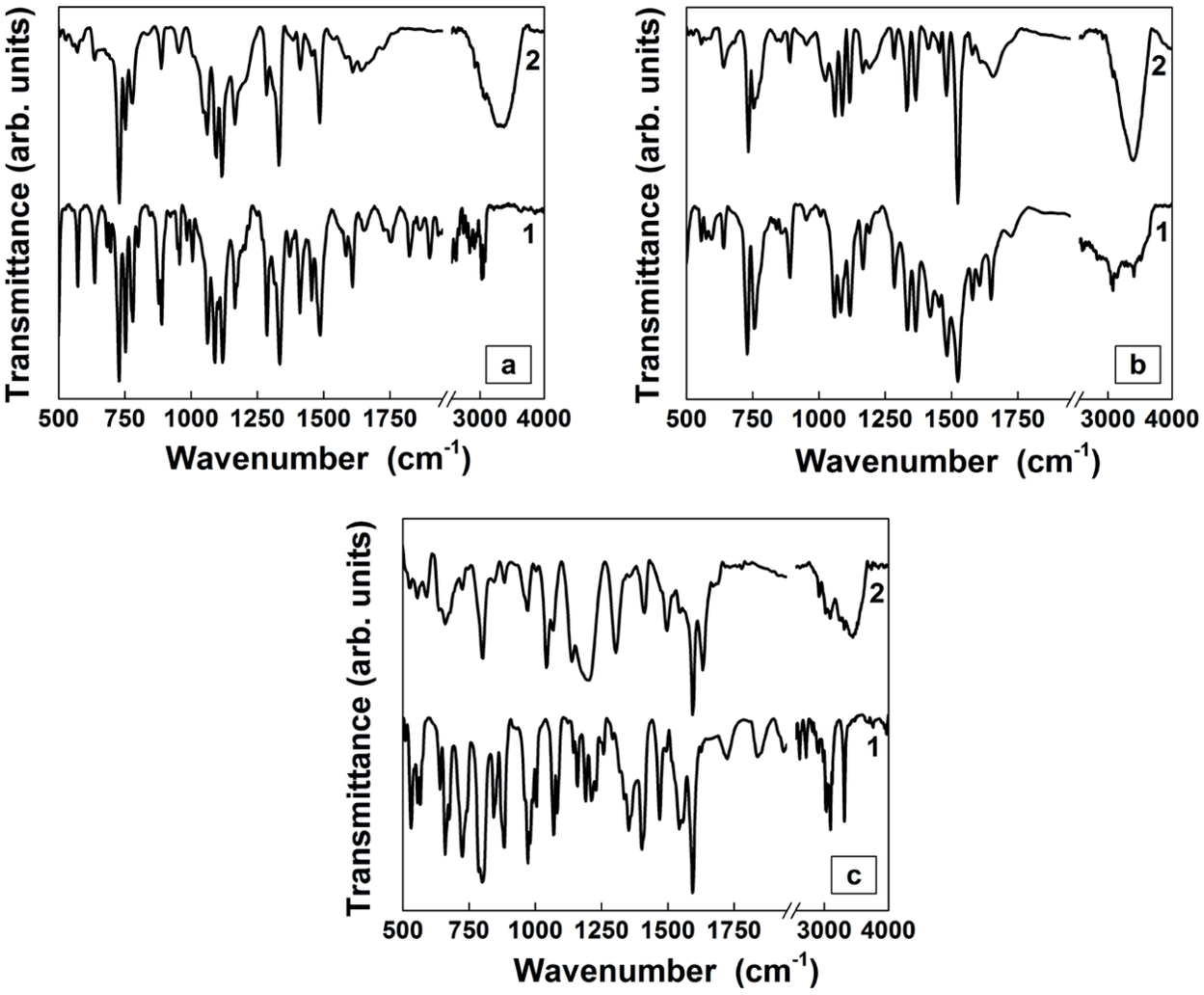

Figure 15. FTIR spectra of the ZnPc (a), MgPc (b) and TPyP (c) as powders (curves 1) and single layers deposited by MAPLE (curves 2).

were identified the vibrations attributed to the C-H out of plane deformation at 725 cm^{-1}, in-plane C-H bend at 754, 1088, 1114 and 1285 cm^{-1}, the C-C stretching in isoindole at 1333 cm^{-1}, the C-C stretching in benzene at 1482 and 1606 cm^{-1}, the C-H bending in aryl at 1490 cm^{-1} [56, 58]. For the TPyP, the following vibrations were attributed: 798 cm^{-1} to the C-H bond in pyrrole, 1500 and 1590 cm^{-1} to the C-C stretching in the pyridyl aromatic ring, 970and 3306 cm^{-1} to porphyrin free-base signature [15].

Based on these results, it can be concluded that no modification appears at the MAPLE transfer of the organic materials.

The UV–VIS spectra (**Figure 16**) of the organic thin films deposited on flexible substrates have identified the absorption maxima typical to the used compounds (**Figure 16**). It can be evidenced the presence of the B and Q bands (between 550 and 750 nm) characteristic to ZnPc and MgPc [62, 63]. Two submaxima are remarked in the Q band due to the π-π^* transition, this band being localised on the phthalocyanine ring [84, 85]. The π-π^* absorption is emphasised

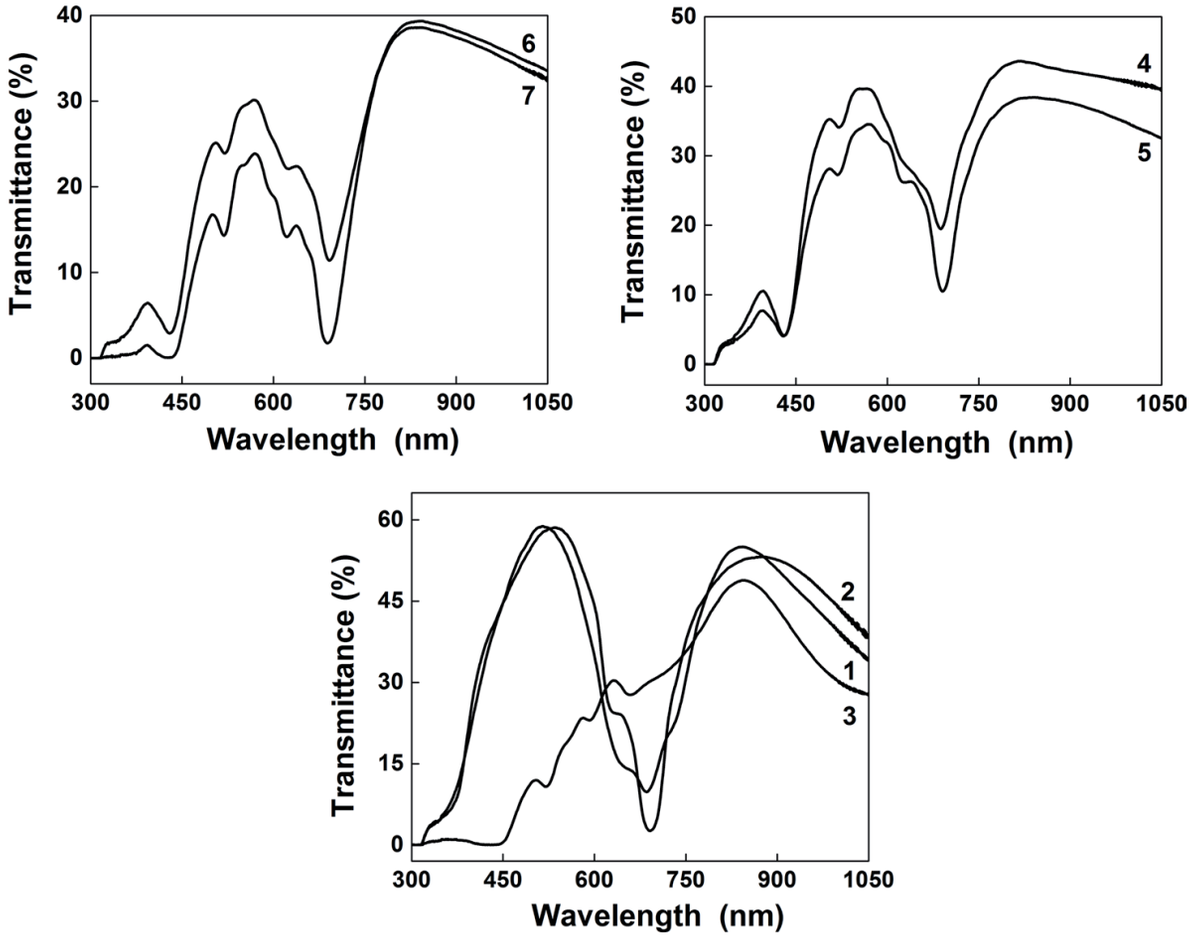

Figure 16. Transmission spectra of the organic layers deposited by MAPLE: single layers—ZnPc (curve 1), MgPc (curve 2), TPyP (curve 3), heterostructures containing stacked films—ZnPc/TPyP (curves 4), MgPc/TPyP (curve 5) and heterostructures with mixed layers—ZnPc:TPyP (curves 6), MgPc:TPyP (curve 7).

also in the TPyP film, being specific to the free-base ethio-type porphyrin, with the B (428 nm) and Q (with maxima at 520, 590 and 660 nm) bands [86].

Investigating the emission properties (at 435 nm excitation wavelength) of the samples based on phthalocyanines and porphyrins was noted that those containing ZnPc present a large emission band (**Figure 17**) with a maximum at 690 nm and those with MgPc show a broader band having the maximum at ~800 nm, associated with the Davidov coupling in the phthalocyanine solid films [84].

An emission band with two maxima at 660 and 713 nm was observed in the TPyP film, these peaks being characteristic to TPyP free base [86]. In the heterostructures prepared with stacked layers, the TPyP emission bands were also evidenced (**Figure 17** curves 4 and 5). For the heterostructures made with blends, a decrease in the emission intensity attributed to TPyP (leading even to its quenching) was observed (**Figure 17**, curves 6 and 7).

Layers based on ZnPc, MgPc and TPyP were successfully transferred by MAPLE on ITO flexible substrates. Only the ZnPc presents a certain crystallinity degree when is deposited both in stacked and blend forms with TPyP, all the others organic films being amorphous.

http://dx.doi.org/10.5772/67702

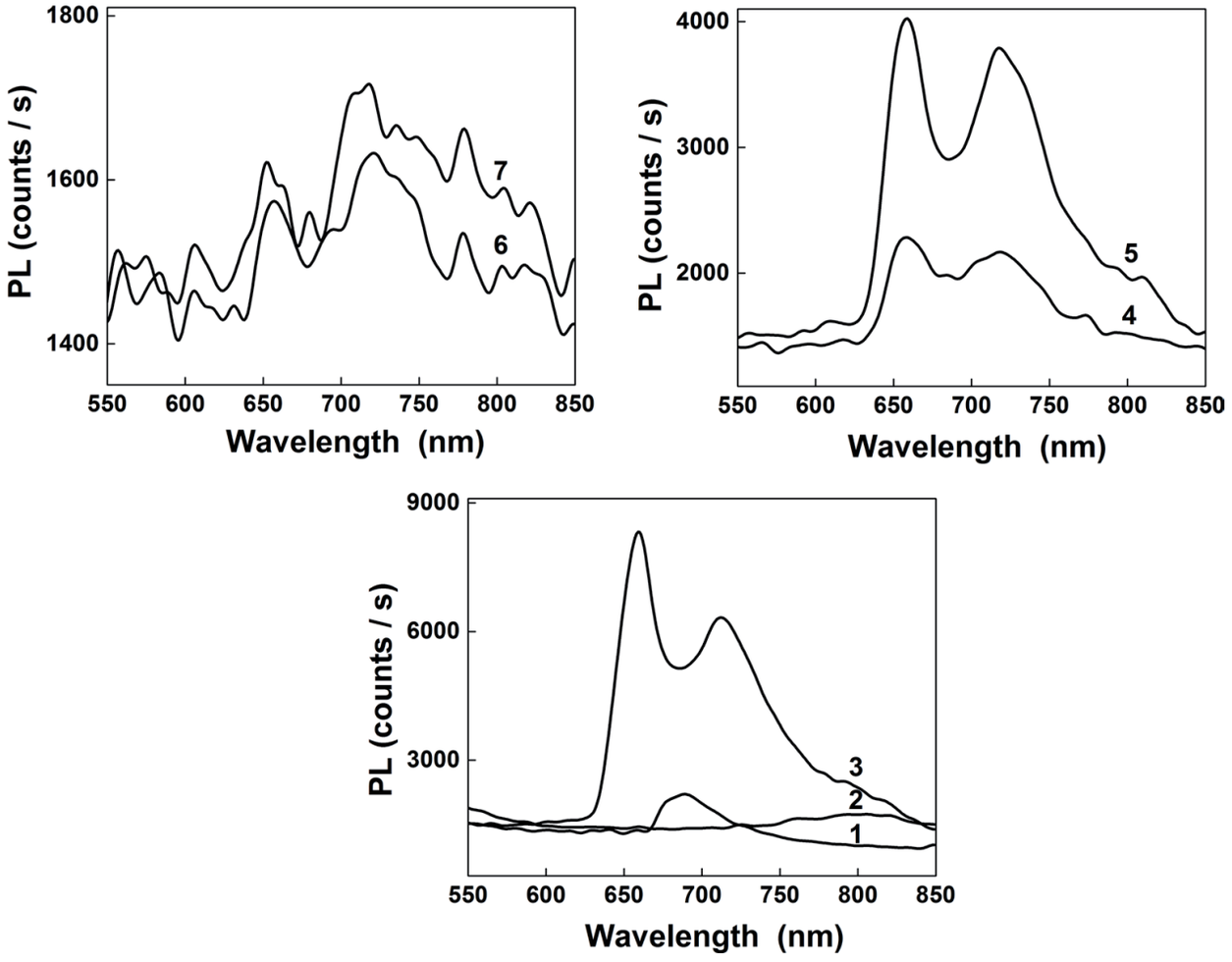

Figure 17. Photoluminescence spectra of the organic layers deposited by MAPLE: single layers—ZnPc (curve 1), MgPc (curve 2), TPyP (curve 3), heterostructures containing stacked films—ZnPc/TPyP (curves 4), MgPc/TPyP (curve 5) and heterostructures with mixed layers—ZnPc:TPyP (curves 6), MgPc:TPyP (curve 7).

The morphology with grains can be attributed also to the phthalocyanines but also to the MAPLE deposition method. The FTIR spectra confirm that the film deposited by MAPLE preserves the vibrational properties of the raw materials. The optical properties of the films evidenced a large absorption domain in the visible range. A quenching of the photoluminescence in the bulk heterostructures was observed.

4. Organic heterostructures based on single and multilayer thin films: electrical properties for device applications

The *I-V* characteristics (**Figure 18**) for the heterostructures prepared by VTE were recorded under dark conditions, in the range of 0V–1V. By using an additional layer of PEDOT:PSS, the current value in the standard structures increased from 1.6×10^{-5} A (glass/ITO/ZnPc/C60/NTCDA/Al) at 6×10^{-4}A (glass/ITO/PEDOT:PSS/ZnPc/C60/NTCDA/Al). This supplementary layer favours the hole injection from the ITO electrode in the first organic film [52].

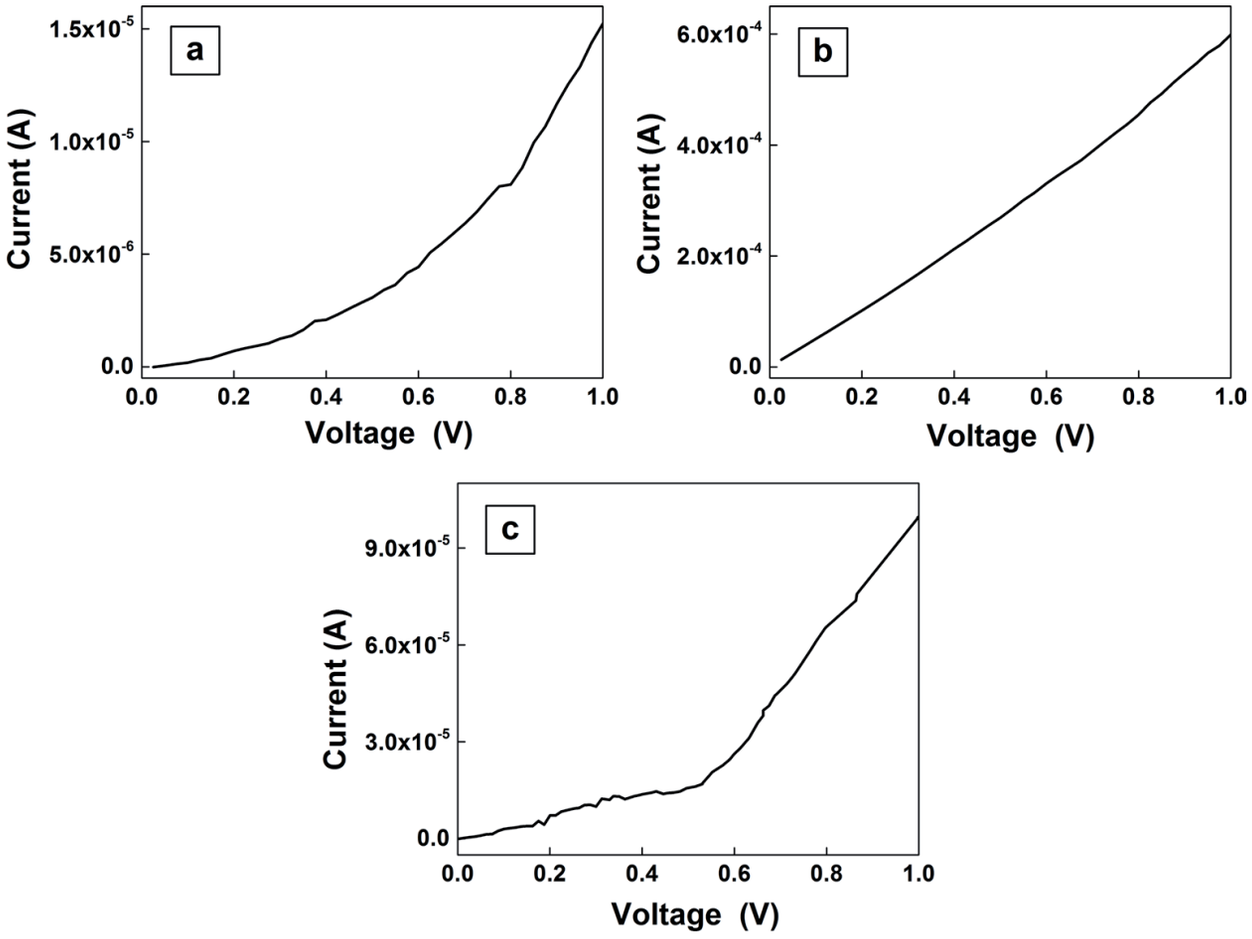

Figure 18. Current-voltage characteristics of the organic heterostructures deposited by VTE: ITO/ZnPc/C60/NTCDA/Al (a), ITO/PEDOT:PSS/ZnPc/C60/NTCDA/Al (b) and glass/Al/NTCDA/C60/ZnPc/ITO (c) structures.

By the deposition of these materials in the inversed order from Al to ITO, an improvement in the current value was also obtained, from 1.6×10^{-5} (glass/ITO/ZnPc/C60/NTCDA/Al) A at 1×10^{-4} A (glass/Al/NTCDA/C60/ZnPc/ITO). Preparing the heterostructure in this way was avoided the interaction of the hot Al atoms with the organic layer which can determine the appearance of some recombination centres at the interface [87].

Thus, the high current values obtained for these heterostructures can be useful for the OPV applications. It was remarked that the current value can be increased either using a supplementary PEDOT:PSS layer or by preparing the heterostructure in the inverted way.

The resistivity for the AZO layers prepared by PLD was determined using a four-point probe method, the values being between 2.7×10^{-4} and 3.2×10^{-4} Ω cm in the case of untreated layers and between 2.5×10^{-4} and 3.1×10^{-4} Ωcm in the case of the treated layers in oxygen plasma (**Table 1**).

For analysis of the NTCDA/ZnPc/AZO structures from electrical point of view, an injection contact behaviour was evidenced for both structures deposited on untreated AZO and treated AZO films (**Figure 19**). 5AZO and 10AZO films were characterised by a lower resistivity compared to that of the untreated AZO layer, and are chosen to facilitate the charge carrier injection. It was observed that the *I-V* characteristics became asymmetric for the heterostructures prepared on

http://dx.doi.org/10.5772/67702

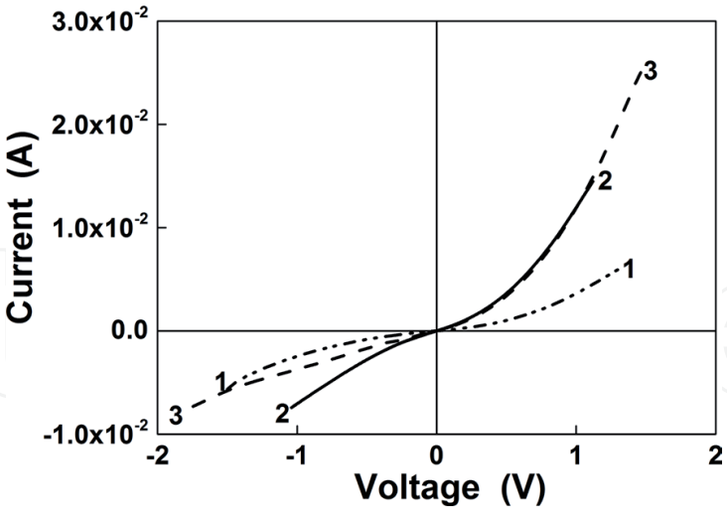

Figure 19. Current-voltage characteristics of the organic heterostructures deposited by MAPLE: AZO/ZnPc/NTCDA/Au structure on substrates untreated (curve 1), treated in oxygen plasma for 5 min (curve 2) and treated in oxygen plasma for 10 min (curve 3).

treated AZO substrates. At low voltages (under 0.4 V), the characteristics are linear and at higher voltages the effect of the space charge limited currents (SCLC) becomes dominant. At direct polarisation, at 1V, the current value increases from 3×10^{-3} A in the structure with AZO at 1.5×10^{-2} A in the structures with 5AZO and 10AZO (**Figure 19** Quadrant 1). An increase in the work function of the AZO electrode was induced by the oxygen plasma treatment [88], having as effect a decrease in the energetic barrier at the AZO/organic interface which improves the injection of the charge carriers from AZO in the organic layer.

Taking into consideration the properties of the AZO, this TCO can be integrated in organic heterostructure, instead of the ITO electrode. The heterostructures prepared on AZO are characterised by current values suitable for the photovoltaic applications. Moreover, treating in oxygen plasma the AZO substrate can be increased the current value in the heterostructures based on ZnPc and NTCDA.

The electrical properties of stacked and blend layers deposited by MAPLE on flexible substrate were also investigated. Regarding the stacked structures, they were energetically favourable, taking into account the ionisation potential (IP) and electron affinity (EA) levels in ZnPc ($E_{IP;ZnPc}$ = 5.28 eV and $E_{EA;ZnPc}$ = 3.28 eV [89]), MgPc ($E_{IP;MgPc}$ = 5.4eV and $E_{EA;MgPc}$ = 3.9 eV [90]) and TPyP ($E_{IP;TPyP}$ = 6.8 eV, $E_{EA;TPyP}$ = 4.1 eV [86]).

The *I-V* characteristics recorded under dark and under illumination conditions, in 0V–1V domain, are near linear (**Figure 20**). In the dark, the higher value of the current (~10^{-6} A) was obtained for the Al/MgPc:TPyP/ITO structure, with ~ 3 orders of magnitude higher than the value presented by the Al/MgPc/TPyP/ITO structure. As was remarked in the AFM images (**Figure 10** g), MgPc:TPyP layer seems to be characterised by a larger roughness which can lead to the formations of some dipoles which reduce the energetic barrier at interfaces favouring the charge transport [83].

An increase in the current value and a photovoltaic effect was also evidenced in the Al/ZnPc:TPyP/ITO structure after exposure to light (**Figure 21**). The solar cell parameters are:

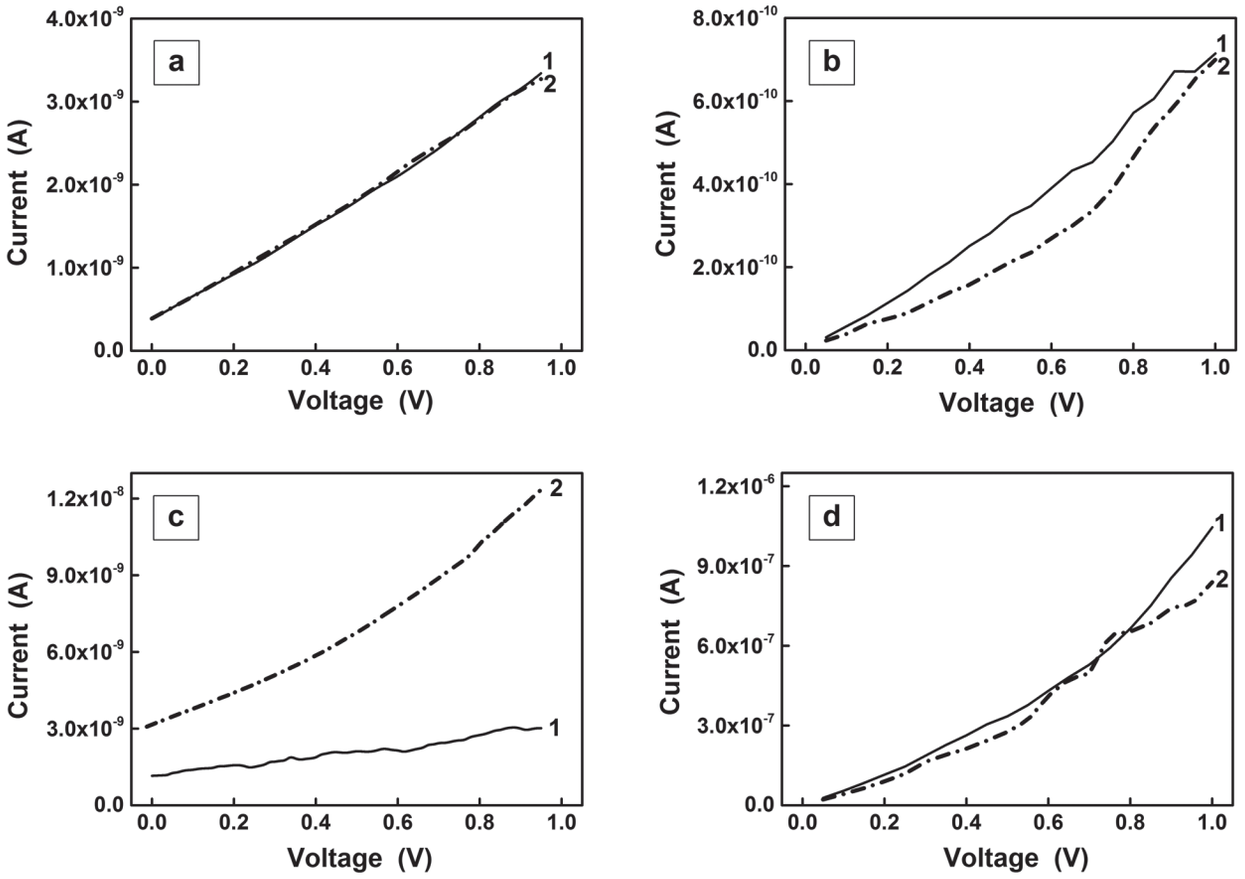

Figure 20. Current-voltage characteristics (in dark conditions—curves 1 and under illumination—curves 2) of the organic heterostructures deposited by MAPLE: PET/ITO/ZnPc/TPyP/Al (a), PET/ITO/MgPc/TPyP/Al (b), PET/ITO/ZnPc:TPyP/Al (c) and PET/ITO/MgPc:TPyP/Al (d) structures.

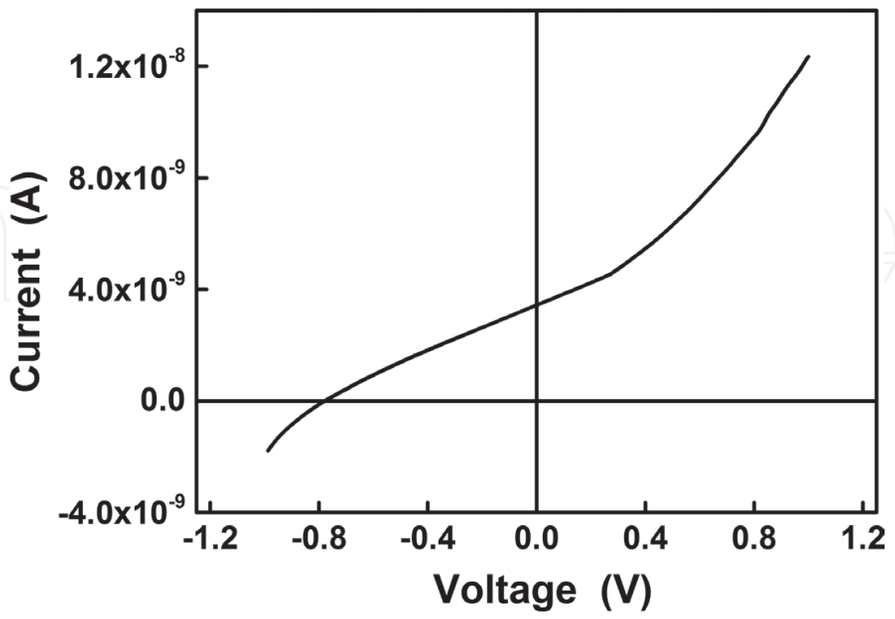

Figure 21. Current-voltage characteristic (under light, −1 V–1 V domain) of the PET/ITO/ZnPc:TPyP/Al heterostructure deposited by MAPLE.

I_{SC} = 3.4 × 10^{-9} A; U_{OC} = 0.77 V and FF = 0.28. Even if in the PL spectra of the MgPc:TPyP structure (**Figure 17**) was remarked a quenching of the photoluminescence, in the *I-V* characteristic recorded under illumination between −1 and 1V, the photovoltaic effect was not evidenced. This means that for this case the collection of the charge carrier at the electrodes has not occurred.

In analysis of the structures prepared with stacked layer, an increased current value was obtained in Al/TPyP/ZnPc/ITO structure comparing to that based on MgPc. This can be explained, considering the position of the HOMO and LUMO levels in these materials, a better hole injection from the ITO electrode in the ZnPc layer being ensured by the lower barrier at the ITO/ZnPc interface (WF_{ITO} = 4.6 eV [91] and $\Delta E_{ZnPc\text{-}ITO}$ = 0.68 eV).

Organic heterostructures based on ZnPc, MgPc and TPyP are suitable to be used in OPV due their electrical properties, especially in bulk forms instead of stacked layers.

5. Conclusions

Heterostructures based on ZnPc were prepared using two different deposition techniques. In a first step, ZnPc was deposited into a multilayer structure in combination with C60 and NTCDA by VTE, the most accessed method for the deposition of organic materials.

The heterostructure were fabricated starting from glass/ITO or glass/ITO covered by a thin film of PEDOT:PSS on which were deposited ZnPc, C60, NTCDA and Al electrode or starting from glass/Al, followed by the deposition of NTCDA, C60, ZnPc and ITO electrode. The structures present the absorption maxima characteristic to the used materials. It was evidenced that the way in which the layers are deposited influenced the properties. *I-V* characteristics revealed that the value of the current is increased in normal configuration glass/ITO/ZnPc/C60/NTCDA/Al when an additional PEDOT:PSS layer is used. An increase in the current value was also achieved depositing the layers in inverted order (glass/Al/NTCDA/C60/ZnPc/ITO).

A p-n heterostructure based on ZnPc and NTCDA layers was also fabricated by a laser technique. Moreover, the structures are obtained on the AZO substrate, and a TCO used to replace the ITO, the material most used as a transparent conductor electrode. AZO layers with adequate optical and electrical properties were prepared by PLD. The influence of an oxygen plasma treatment of AZO on the properties of the organic structures deposited on this TCO was analysed. The UV–VIS spectra show features typical to the used materials, covering a large region of the visible domain. The PL emission bands attributed to the ZnPc and NTCDA were overlapped by the emission bands showed by the AZO substrate. AFM images evidenced a decrease in the size of the grains of the organic heterostructures with the increase in duration of the applied plasma treatment of the AZO substrate. The *I-V* characteristics of the heterostructures revealed an injector contact behaviour and the appearance of the space charge limited currents (characteristic in organic materials) at voltages higher than 0.4V. AZO substrates treated in oxygen plasma (for 5 and 10 min) can favour the injection of the charge carrier in the organic layer, probably as a result of the increasing of AZO work function (leading to a decrease in the energetic barrier at the interface), and determining a current higher with 1 order of magnitude in the heterostructures prepared on the treated substrate.

Organic heterostructures based on metal phthalocyanines and a porphyrin (ZnPc orMgPc and TPyP) were deposited by MAPLE on flexible substrate PET/ITO (in stacked or mixed form). The films preserve their IR absorption properties indicating that no decomposition appears at the laser transfer. The *I-V* characteristics of the heterostructures measured in dark conditions show an increased current value with 3 orders of magnitude higher for the structure with MgPc:TPyP compared to the structure formed with stacked films based on the same compounds. The appearance of the photovoltaic effect was remarked in the heterostructures with ZnPc:TPyP when the structure was exposed to the light.

In conclusion, thin films based on porphyrins and/or phthalocyanines can be deposited in multilayers or blend configurations on various substrates (ITO/glass, AZO/glass, Al/glass or ITO/PET) by different deposition techniques, including laser techniques. The obtained results are promising and very useful for further applications in the photovoltaic field.

Acknowledgements

The work has been funded by the Romanian National Authority for Scientific Research, CNCS-UEFISCDI, projects TE 188/2014, PN-II-RU-TE-2014-4-1590 and the National Authority for Research and Innovation in the frame of Core Program - contract 4N/2016 and contract PN16-480102.

Author details

Marcela Socol[1]*, Nicoleta Preda[1], Anca Stanculescu[1], Florin Stanculescu[2] and Gabriel Socol[3]

*Address all correspondence to: marcela.socol@infim.ro

1 National Institute of Material Physics, Bucharest-Magurele, Romania

2 Faculty of Physics, University of Bucharest, Bucharest-Magurele, Romania

3 National Institute for Lasers, Plasma and Radiation Physics, Bucharest-Magurele, Romania

References

[1] Yu J.S., Yin X.X., Xu Z.S., Deng P., Han Y.B., Zhou B.J., Tang W.H. Bisalkylthio side chain manipulation on two-dimensional benzo[1,2-b:4,5-b′]dithiophene copolymers with deep HOMO levels for efficient organic photovoltaics. Dyes and Pigments. 2017;**136**:312–320. DOI: 10.1016/j.dyepig.2016.08.057

[2] Park Y., Berger J., Tang Z., Muller-Meskamp, L., Lasagni A. F., Vandewal K., Leo K. Flexible, light trapping substrates for organic photovoltaics. Applied Physics Letters. 2016;**109**(9): Article Number: 093301. DOI: 10.1063/1.4962206

[3] Lee S., Kim B., Jung H., Shin H., Lee H., Lee J., Park J. Synthesis and electroluminescence properties of new blue dual-core OLED emitters using bulky side chromophores. Dyes and Pigments. 2017;**136**:255–261. DOI: 10.1016/j.dyepig.2016.08.010

[4] Zhou H., Cheong H. G., Park J. W. Charge carrier transport through the interface between hybrid electrodes and organic materials in flexible organic light emitting diodes. Journal of Nanoscience and Nanotechnology. 2016;**16**(5):5179–5185. DOI: 10.1166/jnn.2016.12265

[5] Xiang L. Y., Ying J., Wang W., Xie W. F. High mobility n-channel organic field-effect transistor based a tetratetracontane interfacial layer on gate dielectrics. IEEE Electron Device Letters. 2016;**37**(12):1632–1635. DOI: 10.1109/LED.2016.2616517

[6] Kheradmand-Boroujeni B., Schmidt G.C., Hoft D., Haase K., Bellmann M., Ishida K., Shabanpour R., Meister T., Carta C., Hubler A. C., Ellinger F. Small-signal characteristics of fully-printed high-current flexible all-polymer three-layer-dielectric transistors. Organic Electronics. 2016;**34**: 275–283. DOI: 10.1016/j.orgel.2016.04.037

[7] Heliatek. Heliatek sets new organic photovoltaic world record efficiency of 13.2% [Internet]. 2016. Available from: http://www.heliatek.com/en/press/press-releases/details/heliatek-sets-new-organic-photovoltaic-world-record-efficiency-of-13-2

[8] Pochettino A. The development of organic conductors, including semiconductors, metals and superconductors cont. Academy Lincei Rendus. 1906;**15**:355.

[9] Volmer M. Different Photoelectric Phenomena in Anthracene, their Relation to one another, to Fluorescence and to the Formation of Dianthracene. Annalen der Physik. 1913;**345**(4):775–796. DOI:10.1002/andp.19133450411

[10] Kearns D., Calvin M. Photovoltaic effect and photoconductivity in laminated organic systems. The Journal of Chemical Physics. 1958;29(4):950–951. dx.doi.org/10.1063/1.1744619

[11] Tang C. W. Two-layer organic photovoltaic cell. Applied Physics Letters. 1986;**48**:183–185. DOI: http://dx.doi.org/10.1063/1.96937

[12] Spanggaard H., Krebs F. C. A brief history of the development of organic and polymeric photovoltaics. Solar Energy Materials & Solar Cells. 2004;**83**:125–146. DOI:10.1016/j.solmat.2004.02.021

[13] Hoppe H., Sariciftci N. S. Organic solar cells: An overview. Journal of Material Research. 2004;**19**(7):1924–1945. DOI: 10.1557/JMR.2004.0252

[14] Walter M. G., Rudine A. B., Wamser C. C. Porphyrins and phthalocyanines in solar photovoltaic cells. Journal of Porphyrins and Phthalocyanines, 2010;**14**:759–792. DOI: 10.1142/S1088424610002689

[15] Fagadar-Cosma E., Enache C., Armeanu I., Fagadar-Cosma G. Comparative investigations of the absorption and fluorescence spectra of tetrapyridylporphyrine and Zn(ii) tetrapyridylporphyrine. Digest Journal of Nanomaterials and Biostructures. 2007;**2**(1):175–183

[16] Yella A., Lee H. W., Tsao H. N., Yi C., Chandiran A. K., Nazeeruddin M. K., Diau E. W., Yeh C. Y., Zakeeruddin S. M., Gra¨tzel M. Porphyrin-sensitized solar cells with cobalt (II/III)-based redox electrolyte exceed 12 percent efficiency. Science. 2011;**334**:629–634. http://dx.doi.org/10.1126/science.1209688

[17] Mathew S., Yella A., Gao P., Humphry-Baker R., Curchod B. F. E., Ashari-Astani N., Tavernelli I., Rothlisberger U., Nazeeruddin Md. K., Grätzel M. Dye-sensitized solar cells with 13% efficiency achieved through the molecular engineering of porphyrin sensitizers. Nature Chemistry. 2014;**6**:242–247.doi:10.1038/nchem

[18] Orns O K. B., Garcia-Lastra J. M., De La Torre G., Himpsel F. J., Rubio d A., Thygesen K. S. Design of two-photon molecular tandem architectures for solar cells by ab initio theory. Chemical Science. 2015;**6**:3018–302. DOI: 10.1039/c4sc03835e

[19] Monti D., Nardis S., Stefanelli M., Paolesse R., Di Natale C., D'Amico A. Porphyrin-based nanostructures for sensing applications. Journal of Sensors. 2009;2009: 1-10. http://dx.doi.org/10.1155/2009/856053

[20] Baran J. D., Grönbeck H., Hellman A. Analysis of porphyrines as catalysts for electrochemical reduction of O_2 and oxidation of H_2O. Journal of American Chemical Society. 2014;**136**(4):1320–1326.DOI: 10.1021/ja4060299

[21] Ishihara S., LabutaJ., Van Rossom W., Ishikawa D., Minami K., Hill J. P., Ariga K. Porphyrin-based sensor nanoarchitectonics in diverse physical detection modes. Physical Chemistry Chemical Physics. 2014;**16**(21):9713–9746. DOI: 10.1039/C3CP55431G

[22] Dougherty T. J., Gomer C. J., Henderson B. W., Jori G., Kessel D., Korbelik M., Moan J., Peng Q. Photodynamic therapy. Journal of the National Cancer Institute. 1998;**90**:889–905. PMC4592754

[23] Huynh E., Leung B. Y. C., Helfield B. L., Shakiba M., Gandier J., Jin C. S., Master E.R., Wilson B. C., Goertz D. E., Zheng G. In situ conversion of porphyrin microbubbles to nanoparticles for multimodality imaging. Nature Nanotechnology. 2015;**10**:325–332. DOI:10.1038/nnano.2015.25

[24] Aviezer D., Cotton S., David M., Segev A., Khaselev N., Galili N., Gross Z., Yayon A. Porphyrin analogues as novel antagonists of fibroblast growth factor and vascular endothelial growth factor receptor binding that inhibit endothelial cell proliferation, tumor progression, and metastasis.Cancer Research.2000;**60**:2973–2980. PubMed ID:**10850445**

[25] Stanculescu A., Socol G., Vacareanu L., Socol M., Rasoga O., Breazu C., Girtan M., Stanculescu F. MAPLE preparation and characterization of mixed arylenevinylene based oligomers: C60 layers. Applied Surface Science. 2016;**374**:278–289. http://dx.doi.org/10.1016/j.apsusc.2015.11.250

[26] Stubinger T., Brutting W. Exciton diffusion and optical interference in organic donor-acceptor photovoltaic cells. Journal of Applied Physics. 2001;**90**:3632–3641.

[27] Peumans P., Forrest S.R. Very-high-efficiency double-heterostructure copper phthalocyanine/C-60 photovoltaic cells. Applied Physics Letters. 2001;79:126–128. DOI: http://dx.doi.org/10.1063/1.1384001

[28] Dao Q.D., Hori T., Fukumura K., Masuda T., Kamikado T., Fujii A., et al. Effects of processing additives on nanoscale phase separation, crystallization and photovoltaic performance of solar cells based on mesogenic phthalocyanine. Organic Electronics. 2016;**14**:2628–2634. http://dx.doi.org/10.1016/j.orgel.2013.05.041

[29] Xue J., Rand B.P., Uchida S., Forrest S.R. A hybrid planar-mixed molecular heterojunction photovoltaic cell. Advanced Materials. 2005;**17**:66–71. DOI: 10.1002/adma.200400617

[30] Xue J., Uchida S., Rand B.P., Forrest S.R. Asymmetric tandem organic photovoltaic cells with hybrid planar-mixed molecular heterojunctions. Applied Physics Letters. 2004;**85**:5757–5759. DOI: http://dx.doi.org/10.1063/1.1829776

[31] Cho K. T., Rakstys K., Cavazzini M., Orlandi S., Pozzi G., Nazeeruddi M. K. Perovskite solar cells employing molecularly engineered Zn(II) phthalocyanines as hole-transporting materials. Nano Energy. 2016;**30**:853–857. http://dx.doi.org/10.1016/j.nanoen.2016.09.008.

[32] Leznoff C. C., Lever A. B. P. (eds.). Phthalocyanines: Properties and Applications : Volume 2, New York: VCH Publishers, 1993, 355p.

[33] Rao S. V., Rao D. N. Excited state dynamics in phthalocyanines studied using degenerate four wave mixing with incoherent light. Journal of Porphyrins Phthalocyanines. 2002;**6** 233–237. DOI: http://dx.doi.org/10.1142/S1088424602000270

[34] Mali S. S., Dalavi D. S., Bhosale P. N., Betty C. A., Chauhancand A. K., Patil P. S. Electro-optical properties of copper phthalocyanines (CuPc) vacuum deposited thin films. RSC Advances. 2012;**2**:2100–2104.DOI: 10.1039/C2RA00670G

[35] Law K. Y. Organic photoconductive materials: recent trends and developments. Chemical Reviews. 1993;**93**(1): 449–486. DOI: 10.1021/cr00017a020

[36] Ghorannevis Z., Akbarnejad E., Elahi A. Salar, Ghoranneviss M. Application of RF magnetron sputtering for growth of AZO on glass substrate. Journal of Crystal Growth. 2016;**447**:62–66. http://dx.doi.org/10.1016/j.jcrysgro.2016.04.062

[37] Socol G., Socol M., Stefan N., Axente E., Popescu-Pelin G., Craciun D., et al. Pulsed laser deposition of transparent conductive oxide thin films on flexible substrate. Applied Surface Science. 2012;**26**0:42–46. DOI:10.1016/j.apsusc.2012.02.14

[38] Kymakis E., Stylianakis M. M., Spyropoulos G. D., Stratakis E., Koudoumas E., Fotakis C. Spin coated carbon nanotubes as the hole transport layer in organic photovoltaics. Solar Energy Materials and Solar Cells. 2012;**96**:298–301: http://dx.doi.org/10.1016/j.solmat.2011.09.046

[39] Xiong K., HouL., Wu M., Huo Y., Mo W., Yuan Y., Sun S.,Xu W., Wang E. From spin coating to doctor blading: A systematic study on the photovoltaic performance of an isoin-

digo-based polymer. Solar Energy Materials and Solar Cells. 2015;**132**:252–259. http://dx.doi.org/10.1016/j.solmat.2014.08.039

[40] Haldar A., Liao K.-S., Curran S. A. Fabrication of inkjet printed organic photovoltaics on flexible Ag electrode with additives. Solar Energy Materials and Solar Cells. 2014;**125**:283–290. http://dx.doi.org/10.1016/j.solmat.2014.03.013

[41] Kim H. Transparent Conducting Oxide Films. In: Easton R., editor. Pulsed Laser Deposition of Thin Films: Applications-Led Growth of Functional Materials. 1st ed. New York, United States: John Wiley & Sons Inc.; 2006, pp. 240–255. DOI: 10.1002/9780470052129.ch11

[42] Norton D. P. Pulsed laser deposition of complex materials: progress toward applications. In: Eason R., editor. Pulsed Laser Deposition of Thin Films: Applications-Led Growth of Functional Materials. 1st ed. New York, United States: Wiley & Sons; 2006, pp. 3–32. DOI: 10.1002/9780470052129.ch1

[43] Socol G., Craciun D., Mihailescu I.N., Stefan N., Besleaga C., Ion L., et al. High quality amorphous indium zinc oxide thin films synthesized by pulsed laser deposition. Thin Solid Films. 2011;**520**:1274–1277. DOI:10.1016/j.tsf.2011.04.196

[44] Thomas M. T. Vacuum deposition techniques. In: G.L. Weissler and Carlson R.W., editors. Methods in Experimental Physics. Volume 14, Vacuum Physics and Technology. New York, Elsevier. 1980, pp.521–575.http://dx.doi.org/10.1016/S0076-695X(08)60385-3

[45] Graper E. B. Resistance evaporation. In: Glocker D. A., Shah S. I., editors. Handbook of Thin Film Process Technology (Inst. Phys. Publ., Bristol 1995) A 1.1: pp.A1.1:1–A1.1:7.

[46] Stanculescu A., Stanculescu F., Tugulea L., Socol M. Optical properties of 3,4,9,10-perylenetetracarboxylic dianhydride and 8-hydroxyquinoline aluminium salt films prepared by vacuum deposition. Material Science Forum. 2006;**514–516**:956–960

[47] Luches A., Caricato A. P. Fundamentals and applications of MAPLE. In: Miotello A., Ossi P. M., editors. Laser-Surface Interactions for New Materials Production. 1st ed. Berlin: Springer Berlin Heidelberg; 2010, pp. 203–233. DOI 10.1007/978-3-642-03307-0_9

[48] Caricato A. P. Lasers in materials science. MAPLE and MALDI: theory and experiments. In: M. Castillejo, M. O., Paolo,L. Zhigilei, editors. Lasers in Materials Science. 1st ed. Switzerland: Springer International Publishing; 2014, pp. 295–323. DOI: 10.1007/978-3-319-02898-9_12

[49] Socol M., Preda N., Vacareanu L., Grigoras M., Socol G., Mihailescu I.N., et al. Organic heterostructures based on arylenevinylene oligomers deposited by MAPLE. Applied Surface Science. 2014;**302**:216–222. DOI: 10.1016/j.apsusc.2013.12.091

[50] Socol M., Preda N., Rasoga O., Breazu C., Stavarache I., Stanculescu F., et al. Flexible heterostructures based on metal phthalocyanines thin films obtained by MAPLE. Applied Surface Science.2016;**374**:403–410. DOI 10.1016/j.apsusc.2015.10.166

[51] Caricato A. P., Cesaria M., Gigli G., Loiudice A., Luches A., Martino M., et al. Poly-(3-hexylthiophene)/6,6 -phenyl-C-61-butyric-acid-methyl-ester bilayer deposition by matrix-assisted pulsed laser evaporation for organic photovoltaic applications. Applied Physics Letters. 2012;**100**:073306. DOI:10.1063/1.3685702

[52] Lin C.-F., Zhang M., Liu S.-W., ChiuT.-L., Lee J.-H. High photoelectric conversion efficiency of metal phthalocyanine/fullerene heterojunction photovoltaic device. International Journal of Molecular Sciences. 2011;**12**: 476–505.doi:10.3390/ijms12010476

[53] Socol M., Rasoga O., Breazu C., Socol G., Preda N., Pasuk I., et al. Heterostructures based on small molecules organic compounds. Digest Journal of Nanomaterials and Biostructures. 2015;**10**(4):1383–1392

[54] Senthilarasu S., Velumani S., Sathyamoorthy R., Subbarayan A., Ascencio J.A., Canizal G., et al. Characterization of zinc phthalocyanine (ZnPc) for photovoltaic applications. Applied Physics A-Materials Science & Proces. 2003;**77**(3–4):383–389. DOI: 10.1007/s00339-003-2184-7

[55] Ginzburg B. M., Tulchiev Sh., Tabarov S. K., Shepelevski A. A., Shibaev L. A. X-ray diffraction analysis of C[sub 60] fullerene powder and fullerene soot. Technical Physics. 2005;**50**(11):1458. DOI 10.1134/1.2131953

[56] Gaffo L., Cordeiro M.R., Freitas A.R., Moreira W.C., Girotto E. M., Zucolotto V. The effects of temperature on the molecular orientation of zinc phthalocyanine films. Journal of Material Science. 2010;**45**:1366–1370. DOI:10.1007/s10853-009-4094-3

[57] Zhang H., Wu C., Liang L., Chen Y., He Y., Zhu Y., et al. Structural, morphological and optical properties of C_{60} cluster thin films produced by thermal evaporation under argon gas. Journal of Physics: Condensed Matter. 2001;**13**(13):2883–2889

[58] Seoudi R., El-Bahy G.S., El Sayed Z.A. FTIR, TGA and DC electrical conductivity studies of phthalocyanine and its complexes. Journal of Molecular Structure. 2005;**753**(1):119–126. http://dx.doi.org/10.1016/j.molstruc.2005.06.003

[59] Triboni E. R., da Silva M. F. P., Finco A. T., Rodrigues M. A., Demets G. J.-F., Dyszy F. H., et al. Synthesis and properties of new paramagnetic hybrid bayerite from Al(0)/naphthalene dianhydride reaction. Materials Research. 2010;**13**(4):505–511.

[60] Braatz C. R., Ohl G., Jakob P. Vibrational properties of the compressed and the relaxed 1,4,5,8-naphthalene-tetracarboxylic dianhydride monolayer on Ag(111). The Journal of Chemical Physics. 2012;**136**(13):134706. DOI: http://dx.doi.org/10.1063/1.3699030.

[61] Torsi L., Dodabalapur A., Cioffi N., Sabbatini L., Zambonin P.G. NTCDA organic thin-film-transistor as humidity sensor: weaknesses and strengths. Sensors and Actuators B. 2001;**77**(1–2):7–11. http://dx.doi.org/10.1016/S0925-4005(01)00664-5

[62] Sathyamoorthy R., Senthilarasu S. Influence of RMS strain on optical band gap of Zinc Phthalocyanine (ZnPc) thin films. Solar Energy. 2006;**80**:201–208. http://dx.doi.org/10.1016/j.solener.2005.06.005

[63] Senthilarasu S., Hahn Y.B., Lee S.H. Structural analysis of zinc phthalocyanine (ZnPc) thin films: X-ray diffraction study. Journal of Applied Physics. 2007;**102**(4):043512. DOI: http://dx.doi.org/10.1063/1.2771046

[64] Jayatissa A. H., Nadarajah A., Dutta A.K. Investigation of C_{60} films for surface finishing applications. Proceeding SPIE. 2005;**6002**:60021A-1. doi:10.1117/12.631051

[65] Chu C.-W., Shao Y., Shrotriya V., Yang Y. Efficient photovoltaic energy conversion in tetracene-C60 based heterojunctions. Applied Physics Letters. 2005;**86**,243506. DOI: 10.1063/1.1946184

[66] Tachikawa H., Kawabata H., Miyamoto R., Nakayama K., Yokoyama M. Experimental and theoretical studies on the organic–inorganic hybrid compound: aluminum-NTCDA co-deposited film. The Journal of Physical Chemistry B. 2005;**109**(8):3139–3145. DOI: 10.1021/jp046168e

[67] Dong B.-Z., Fang G.-J., Wang J.-F., Guan W.-J., Zhao X.-Z. Effect of thickness on structural, electrical, and optical properties of ZnO: Al films deposited by pulsed laser deposition. Journal of Applied Physics. 2007;**101**(3):033713. DOI: http://dx.doi.org/10.1063/1.2437572

[68] Kim H., Gilmore C. M., Horwitz J. S., Piqué A., Murata H., Kushto G. P., et al. Transparent conducting aluminum-doped zinc oxide thin films for organic light-emitting devices. Applied Physics Letters. 2000;**76**(3):259. DOI: http://dx.doi.org/10.1063/1.125740

[69] Wu H.-W., Yang R.-Y., Hsiung C.-M., Chu C.-M. Characterization of aluminum-doped zinc oxide thin films by RF magnetron sputtering at different substrate temperature and sputtering power. Journal of Materials Science: Materials in Electronics. 2013;**24**(1):166–171. DOI: 10.1007/s10854-012-0769-7

[70] Stanculescu A., Socol M., Rasoga O., Mihailescu I. N., Socol G., Preda N., et al. Laser prepared organic hetrostructures on glass/AZO substrates. Applied Surface Science. 2014;**302**:169–176. http://dx.doi.org/10.1016/j.apsusc.2014.01.181

[71] Martins R., Fortunato E., Nunes P., Ferreira I., Marques A., Bender M. Zinc oxide as an ozone sensor. Journal of Applied Physics. 2004;**96**: 1398–1408. DOI: http://dx.doi.org/10.1063/1.1765864

[72] Chou Y.-H., Yan J.-T., Lee H.-Y., Lee C.-T. AZO films with Al nano-particles to improve the light extraction efficiency of GaN-based light-emitting diodes Proceeding SPIE. 2008;**6894**:68941C.1–68941C.6. DOI: 10.1117/12.765633

[73] Wojdyla M., Derkowska B., Lukasiak Z., W. Bala. Absorption and photoreflectance spectroscopy of zinc phthalocyanine (ZnPc) thin films grown by thermal evaporation. Materials Letters. 2006;**60**(29–30):3441–3446. http://dx.doi.org/10.1016/j.matlet.2006.03.029

[74] Forrest S.R., Holmes R. Organic Polariton Laser Patents. US 20050195874 A1. http://www.google.de/patents/US20050195874.

[75] Ding J., Chen H., Zhao X., Ma S. Effect of substrate and annealing on the structural and optical properties of ZnO: Al films. Journal of Physics and Chemistry of Solids. 2010;**71**(3):346–350. DOI: 10.1016/j.jpcs.2009.12.088

[76] Ding J.J., Ma S.Y., Chen H.X., Shi X.F., Zhou T.T., Mao L.M. Influence of Al-doping on the structure and optical properties of ZnO films. Physica B: Condensed Matter. 2009;**404**(16): 2439–2443. DOI: 10.1016/j.physb.2009.05.006

[77] Ahn K., Jeong Y.S., Lee H.U., Jeong S.Y., Ahn H.S., Kim H.S., et al. Physical properties of hydrogenated Al-doped ZnO thin layer treated by atmospheric plasma with oxygen gas. Thin Solid Films. 2010;**518**(14):4066–4070. DOI: 10.1016/j.tsf.2010.02.028

[78] Wojdyla M., Bala W., Derkowska B., Lukasiak Z., Czaplicki R., Sofiani Z., et al. Photoluminescence and third harmonic generation in ZnPc thin films. Nonlinear Optics Quantum Optics. 2006;**35**:103–119.

[79] Ng A.M.C., Djurisic A.B., Chan W.K. Organic luminescent nanowires: fabrication and characterization. Proceeding SPIE. 2007;**6828**:682807.1–682807.10. DOI:10.1117/12.760844

[80] Shoheen S. E., Brabec C. J., Sariciftci N. S., Padinger F., Fromherz J., Hummelen J. C. 2.5% efficient organic plastic solar cells. Applied Physics Letters. 2001;**78**(6):841–843. DOI: http://dx.doi.org/10.1063/1.1345834

[81] Zhang C., Hu Y., Tang A., Deng Z., Teng F. Investigating the reduction in the absorption intensity of P3HTin polymer/fullerene "bilayers" coated using orthogonal solvents. Journal of Applied Polymer Science. 2015;**132**(14):41757.DOI: 10.1002/app.41757

[82] El-Nahass M. M., Atta A. A., El-Sayed H. E. A., El-Zaidia E. F. M. Structural and optical properties of thermal evaporated magnesium phthalocyanine (MgPc) thin films. Applied Surface Science. 2008;**254**(8):2458–2465. http://dx.doi.org/10.1016/j.apsusc.2007.09.064

[83] Stanculescu A., Socol M., Socol G., Mihailescu I. N., Girtan M., Stanculescu F. Maple prepared organic heterostructures for photovoltaic application. Applied Physics A: Materials Science & Processing. 2011;**104** (3):921–928. DOI: 10.1007/s00339-011-6440-y

[84] Bala W., Wojdyla M., Rebarz M., Szybowic M., Drozdowski M., Grodzicki A., et al. Influence of central metal atom in MPc (M = Cu, Zn, Mg, Co) on Raman, FT-IR, absorbance, reflectance, and photoluminescence spectra. Journal of Optoelectronic and Advanced Materials. 2009;**11**(3):264–269.

[85] Gu D., Chen Q., Shu J., Tang X., Gan F., Shen S., et al. Optical recording performance of thin films of phthalocyanine compounds. Thin Solid Films. 1995;**257**(1):88–93. http://dx.doi.org/10.1016/0040-6090(94)06327-3

[86] Socol M., Rasoga O., Stanculescu F., Girtan M., Stanculescu A. Effect of the morphology on the optical and electrical properties of TPyP thin films deposited by vacuum evaporation. Optoelectronic Advanced Materials. 2010;**4**(12):2032–2038.

[87] Vogel M., Doka S., Breyer Ch., Lux-Steiner M. Ch., Fostiropoulos K. On the function of a bath ocuproine buffer layer in organic photovoltaic cells. Applied Physics Letters. 2006;**89**:163501–3. DOI: 10.1063/1.2362624

[88] Park Y.S., Seo M., Yi J., Lim D., Lee J. Characteristics of aluminum-doped zinc oxide films with oxygen plasma treatment for solar cell applications. Thin Solid Films. 2013;**547**:47–51. http://dx.doi.org/10.1016/j.tsf.2013.05.065

[89] Stanculescu A., Stanculescu F., Socol M., Grigorescu O. Electrical transport in crystalline perylene derivatives films for electronic devices. Solid State Sciences. 2008;**10**(12):1762–1767. http://dx.doi.org/10.1016/j.solidstatesciences.2008.03.023

[90] Breeze A. J., Salomon A., Ginley D. S., Gregg B. A., Tillmann H., Hörhold H.-H. Polymer-perylenediimide heterojunction solar cells. Applied Physics Letters. 2002;**81**(16):3085–3087. DOI: http://dx.doi.org/10.1063/1.1515362

[91] Cui J., Wang A., Edleman N.L., Ni J., Lee P., Armstrong N.R., et al. Indium tin oxide alternatives-high work function transparent conducting oxides as anodes for organic light-emitting diodes. Advanced Materials. 2001;**13**(19):1476–1480. DOI: 10.1002/1521-4095(200110)13:19<1476::AID-ADMA1476>3.0.CO;2-Y

IntechOpen